BI-TP 2010/42

Intermediate distance correlators in hot Yang-Mills theory

M. Laine[a], M. Vepsäläinen[b], A. Vuorinen[a]

[a] *Faculty of Physics, University of Bielefeld, D-33501 Bielefeld, Germany*

[b] *Department of Physics, P.O.Box 64, FI-00014 University of Helsinki, Finland*

Abstract

Lattice measurements of spatial correlation functions of the operators FF and $F\tilde{F}$ in thermal SU(3) gauge theory have revealed a clear difference between the two channels at "intermediate" distances, $x \sim 1/\pi T$. This is at odds with the AdS/CFT limit which predicts the results to coincide. On the other hand, an OPE analysis at short distances ($x \ll 1/\pi T$) as well as effective theory methods at long distances ($x \gg 1/\pi T$) suggest differences. Here we study the situation at intermediate distances by determining the time-averaged spatial correlators through a 2-loop computation. We do find unequal results, however the numerical disparity is small. Apart from theoretical issues, a future comparison of our results with time-averaged lattice measurements might also be of phenomenological interest in that understanding the convergence of the weak-coupling series at intermediate distances may bear on studies of the thermal broadening of heavy quarkonium resonances.

November 2010

1. Introduction

Spatial correlation functions of local gauge-invariant operators (such as components of the energy-momentum tensor or various charge densities) offer a set of observables that can yield a detailed characterization of the physical properties of a thermal system. Consequently, in lattice QCD, correlators related to gluonic (flavour-singlet) as well as hadronic (flavour non-singlet) operators have been studied since dawn [1, 2] and continue to be important in the present era of unquenched simulations (see, e.g., refs. [3, 4]).

At high temperatures ($T \gg 200$ MeV), spatial correlation functions can be sensitive to different types of physics at different distance scales. At short distances ($x \ll 1/\pi T$), we expect them to display vacuum-like behaviour; at intermediate distances ($x \sim 1/\pi T$), we expect a complicated functional form with thermal modifications of order unity; at long distances ($x \gg 1/\pi T$), the correlators should ultimately reduce to a single exponential, characterized by collective phenomena such as colour-electric or colour-magnetic screening [5]. In addition, the zero-temperature confinement scale may also make an appearance, if a measurement at a low temperature is subtracted from the high-temperature measurement in an effort to remove the vacuum-like behaviour at short distances.

For future reference, we note that the distance scale that one is interested in may influence some technical details of the lattice measurement carried out. For instance, for short-distance physics a signal may be obtained from point-point correlators, whereas the long-distance asymptotics can perhaps best be extracted by using operators averaged over the Euclidean time direction as well as over the transverse spatial plane.

In the present paper, following a recent high-precision lattice measurement [6], we consider spatial correlators within pure SU(3) gauge theory at a temperature above that of the deconfinement transition. The operators correlated are $\mathrm{Tr}\,[F_{\mu\nu}F_{\mu\nu}]$ (corresponding physically to the trace of the energy-momentum tensor, modulo a coefficient) and $\mathrm{Tr}\,[F_{\mu\nu}\tilde{F}_{\mu\nu}]$ (corresponding physically to topological charge density, modulo a coefficient). We assume the operators to be averaged over the Euclidean time coordinate but to remain point-like in space coordinates. On this point we actually differ from ref. [6] in which the operators were point-like also in time; apart from technical simplifications, our choice is motivated by the fact that the correlators then become more analogous to Polyakov-loop ones which are relevant for the phenomenology of heavy quarkonium physics (the ramifications in this direction will be discussed in the conclusions). Time-averaged correlators are also the ones containing the thermodynamic information relevant for spectral sum rules (see, e.g., refs. [7, 8]).

One of the main findings of ref. [6] was that, once the (genuine) vacuum part was subtracted from the correlators, the two channels showed strikingly different behaviours at intermediate distances (cf. fig. 5 of ref. [6]): for $\mathrm{Tr}\,[F_{\mu\nu}F_{\mu\nu}]$ the thermal modification was negative in this range (reducing the correlator) whereas for $\mathrm{Tr}\,[F_{\mu\nu}\tilde{F}_{\mu\nu}]$ it was positive (enhancing the

correlator). That such a difference exists is in contrast with the strongly-coupled AdS/CFT limit of $\mathcal{N} = 4$ Super-Yang-Mills theory which predicts the two correlators to coincide [9, 6].

Within pure SU(3) theory, the emergence of a qualitative difference between the two channels has previously been understood both in the short-distance ($x \ll 1/\pi T$) and in the long-distance ($x \gg 1/\pi T$) limits. In the short-distance limit, the correlators can be expanded in an Operator Product Expansion (OPE). The leading terms are vacuum-like contributions, which already differ as far as non-logarithmic terms are concerned [10]. Furthermore, OPE contributions proportional to the expectation value of the trace anomaly, $(e-3p)(T)$, come with opposite signs [11, 12], underlining that any breaking of conformal invariance is bound to lift the degeneracy.

On the long-distance side ($x \gg 1/\pi T$), the very fact that the two operators have different discrete quantum numbers has been exploited for *defining* colour-electric and colour-magnetic screening masses in a non-Abelian theory [5]. The colour-electric channel couples to $\mathrm{Tr}\,[F_{\mu\nu}\tilde{F}_{\mu\nu}]$ and the colour-magnetic to $\mathrm{Tr}\,[F_{\mu\nu}F_{\mu\nu}]$. Practical measurements in pure Yang-Mills theory and QCD (making use of an infrared effective field theory) can be found in ref. [13] and indeed show substantial variation in the screening masses; the qualitative differences in the corresponding weak-coupling expressions have been elaborated upon in ref. [14].

The purpose of the present paper is to "interpolate" between the known short-distance and long-distance limits, by considering intermediate distances $x \sim 1/\pi T$. This situation is "simple" in the sense that straightforward perturbation theory is formally applicable, without the need of re-organization in terms of OPE or of effective field theories. The challenge is that the correlators have a relatively complicated functional form. Nevertheless, we have managed to obtain expressions for both correlators, and foresee an opportunity for a practical comparison of the weak-coupling expansion against lattice simulations of the type in ref. [6].

The plan of this paper is the following. The observables considered are specified in sec. 2, and the main steps of the computation are described in some detail in sec. 3. Section 4 collects together the basic results applicable for short and intermediate distances, whereas in sec. 5 we elaborate on how the perturbative expressions need to be resummed in the long-distance limit. Numerical illustrations comprise sec. 6, and our conclusions are collected in sec. 7.

2. Setup

Our basic notation follows ref. [12], so we discuss the setup only briefly. We consider pure SU($N_{\rm c}$) Yang-Mills theory (with $N_{\rm c} = 3$ in numerical estimates), dimensionally regularized by analytically continuing to $D = 4 - 2\epsilon$ space-time dimensions ($S_{\rm E} = \int_0^\beta \mathrm{d}\tau \int \mathrm{d}^{3-2\epsilon}\mathbf{x}\, \frac{1}{4} F^a_{\mu\nu} F^a_{\mu\nu}$). The operators considered are

$$\theta \equiv c_\theta\, g_{\rm B}^2 F^a_{\mu\nu} F^a_{\mu\nu} \;, \quad \chi \equiv c_\chi\, \epsilon_{\mu\nu\rho\sigma} g_{\rm B}^2 F^a_{\mu\nu} F^a_{\rho\sigma} \;, \tag{2.1}$$

where $g_{\rm B}^2$ is the bare gauge coupling squared; these operators require no renormalization at the order of our computation. We do not need to specify the coefficients c_θ, c_χ, but note that in ref. [6] the values $c_\theta \approx -\frac{b_0}{2}$, $c_\chi \equiv \frac{1}{64\pi^2}$ were chosen, where $b_0 \equiv \frac{11 N_{\rm c}}{3(4\pi)^2}$. The bare gauge coupling squared can be expanded in terms of the renormalized one, g^2, as

$$g_{\rm B}^2 = g^2 \Lambda^{2\epsilon} \biggl[1 - \frac{11 g^2 N_{\rm c}}{3(4\pi)^2} \frac{1}{\epsilon} + \ldots \biggr] \;, \tag{2.2}$$

where Λ denotes a scale parameter. The $\overline{\rm MS}$ scheme renormalization scale is denoted by $\bar\Lambda^2 \equiv 4\pi \Lambda^2 e^{-\gamma_{\rm E}}$. In order to avoid unnecessary clutter all appearances of $\Lambda^{2\epsilon}$, which cancel when the result is expressed in terms of the renormalized gauge coupling, will be suppressed.

We wish to evaluate the behaviour of the correlators of θ and χ as functions of the spatial distance $x \equiv |\mathbf{x}|$, integrated over the Euclidean time τ. To this end, we define the quantities ($X \equiv (\tau, \mathbf{x})$; $P \equiv (p_n, \mathbf{p})$; $G_\theta(X) \equiv \langle \theta(X) \theta(0) \rangle_{\rm c}$; $G_\chi(X) \equiv \langle \chi(X) \chi(0) \rangle$)

$$\bar G_\theta(x) \equiv \int_0^\beta {\rm d}\tau \, G_\theta(X) \;, \quad \bar G_\chi(x) \equiv \int_0^\beta {\rm d}\tau \, G_\chi(X) \;. \tag{2.3}$$

Using the corresponding Fourier transforms

$$\tilde G_\theta(P) \equiv \int_X e^{-iP\cdot X} G_\theta(X) \;, \quad \tilde G_\chi(P) \equiv \int_X e^{-iP\cdot X} G_\chi(X) \;, \tag{2.4}$$

we see that for our purposes it suffices to consider the static ($p_n = 0$) limit of the correlators in momentum space:

$$\bar G_\theta(x) = \int_{\mathbf{p}} e^{i\mathbf{p}\cdot\mathbf{x}} \, \tilde G_\theta(p_n = 0, \mathbf{p}) \;, \quad \bar G_\chi(x) = \int_{\mathbf{p}} e^{i\mathbf{p}\cdot\mathbf{x}} \, \tilde G_\chi(p_n = 0, \mathbf{p}) \;. \tag{2.5}$$

We work up to next-to-leading order (NLO) in perturbation theory. A natural starting point for the computation are then the expressions in eqs. (3.1) and (3.2) of ref. [12], obtained after "scalarizing" the 1-loop and 2-loop Feynman graphs (fig. 1) contributing to the momentum-space correlators ($d_A \equiv N_{\rm c}^2 - 1$):

$$\begin{aligned} \frac{\tilde G_\theta(P)}{4 d_A c_\theta^2 g_{\rm B}^4} &= (D-2) \biggl[-\mathcal{J}_{\rm a} + \frac{1}{2} \mathcal{J}_{\rm b} \biggr] \\ &+ g_{\rm B}^2 N_{\rm c} \biggl\{ 2(D-2) \Bigl[-(D-1)\mathcal{I}_{\rm a} + (D-4)\mathcal{I}_{\rm b} \Bigr] + (D-2)^2 \Bigl[\mathcal{I}_{\rm c} - \mathcal{I}_{\rm d} \Bigr] \\ &\quad + \frac{22-7D}{3} \mathcal{I}_{\rm f} - \frac{(D-4)^2}{2} \mathcal{I}_{\rm g} + (D-2) \Bigl[-3\mathcal{I}_{\rm e} + 3\mathcal{I}_{\rm h} + 2\mathcal{I}_{\rm i} - \mathcal{I}_{\rm j} \Bigr] \biggr\} \;, \end{aligned} \tag{2.6}$$

$$\begin{aligned} \frac{\tilde G_\chi(P)}{-16 d_A c_\chi^2 g_{\rm B}^4 (D-3)} &= (D-2) \biggl[-\mathcal{J}_{\rm a} + \frac{1}{2} \mathcal{J}_{\rm b} \biggr] \\ &+ g_{\rm B}^2 N_{\rm c} \biggl\{ 2(D-2) \Bigl[-\mathcal{I}_{\rm a} + (D-4)\mathcal{I}_{\rm b} \Bigr] + (D-2)^2 \Bigl[\mathcal{I}_{\rm c} - \mathcal{I}_{\rm d} \Bigr] \\ &\quad - \frac{2D^2 - 17D + 42}{3} \mathcal{I}_{\rm f} - 2(D-4)\mathcal{I}_{\rm g} + (D-2) \Bigl[-3\mathcal{I}_{\rm e} + 3\mathcal{I}_{\rm h} + 2\mathcal{I}_{\rm i} - \mathcal{I}_{\rm j} \Bigr] \biggr\} \;. \end{aligned} \tag{2.7}$$

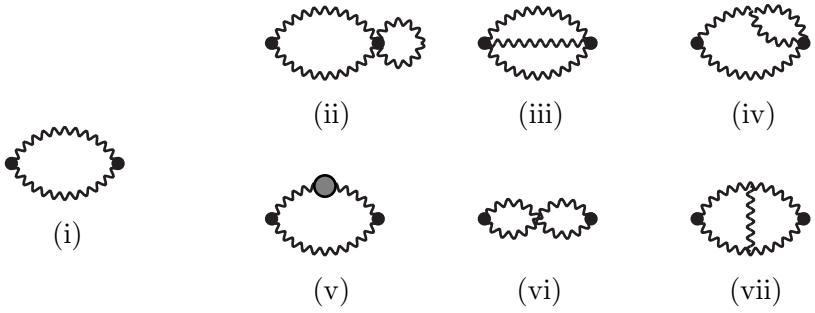

Figure 1: The LO and NLO Feynman graphs contributing to the correlators of eqs. (2.6), (2.7).

The definitions of the master sum-integrals $\mathcal{J}_{\rm a} \ldots \mathcal{I}_{\rm j}$ can be found in eqs. (3.1)–(3.13) below.

It will become clear later on that at long distances, the NLO corrections can overtake the leading order (LO) terms, indicating a breakdown of the perturbative series. In this situation perturbation theory needs to be resummed through effective field theory techniques. We return to when this happens in sec. 5; for the moment we simply compute the correlators as they stand in eqs. (2.5)–(2.7). The results will be denoted by $\bar{G}^{\rm F}_{\theta,\chi}$, with "F" standing for "full theory".

3. Naive full theory computation

In this section, we describe in some detail the evaluation of the various master sum-integrals appearing in eqs. (2.6), (2.7), once they are Fourier transformed according to eq. (2.5).

3.1. Sum-integrals

The master sum-integrals are defined using dimensional regularization in $D = 4 - 2\epsilon$ dimensions and, as in ref. [12], read ($\sum\!\!\!\!\!\!\int_Q \equiv T\sum_{q_n}\int_{\mathbf{q}}$)

$$\mathcal{J}_{\rm a} \equiv \sum\!\!\!\!\!\!\int_Q \frac{P^2}{Q^2}\,, \tag{3.1}$$

$$\mathcal{J}_{\rm b} \equiv \sum\!\!\!\!\!\!\int_Q \frac{P^4}{Q^2(Q-P)^2}\,, \tag{3.2}$$

$$\mathcal{I}_{\rm a} \equiv \sum\!\!\!\!\!\!\int_{Q,R} \frac{1}{Q^2R^2}\,, \tag{3.3}$$

$$\mathcal{I}_{\rm b} \equiv \sum\!\!\!\!\!\!\int_{Q,R} \frac{P^2}{Q^2R^2(R-P)^2}\,, \tag{3.4}$$

$$\mathcal{I}_{\rm c} \;\equiv\; \sum\!\!\!\!\!\!\int_{Q,R} \frac{P^2}{Q^2R^4} \;, \tag{3.5}$$

$$\mathcal{I}_{\rm d} \;\equiv\; \sum\!\!\!\!\!\!\int_{Q,R} \frac{P^4}{Q^2R^4(R-P)^2} \;, \tag{3.6}$$

$$\mathcal{I}_{\rm e} \;\equiv\; \sum\!\!\!\!\!\!\int_{Q,R} \frac{P^2}{Q^2R^2(Q-R)^2} \;, \tag{3.7}$$

$$\mathcal{I}_{\rm f} \;\equiv\; \sum\!\!\!\!\!\!\int_{Q,R} \frac{P^2}{Q^2(Q-R)^2(R-P)^2} \;, \tag{3.8}$$

$$\mathcal{I}_{\rm g} \;\equiv\; \sum\!\!\!\!\!\!\int_{Q,R} \frac{P^4}{Q^2(Q-P)^2R^2(R-P)^2} \;, \tag{3.9}$$

$$\mathcal{I}_{\rm h} \;\equiv\; \sum\!\!\!\!\!\!\int_{Q,R} \frac{P^4}{Q^2R^2(Q-R)^2(R-P)^2} \;, \tag{3.10}$$

$$\mathcal{I}_{\rm i} \;\equiv\; \sum\!\!\!\!\!\!\int_{Q,R} \frac{(Q-P)^4}{Q^2R^2(Q-R)^2(R-P)^2} \;, \tag{3.11}$$

$$\mathcal{I}_{\rm i'} \;\equiv\; \sum\!\!\!\!\!\!\int_{Q,R} \frac{4(Q\cdot P)^2}{Q^2R^2(Q-R)^2(R-P)^2} \;, \tag{3.12}$$

$$\mathcal{I}_{\rm j} \;\equiv\; \sum\!\!\!\!\!\!\int_{Q,R} \frac{P^6}{Q^2R^2(Q-R)^2(Q-P)^2(R-P)^2} \;. \tag{3.13}$$

As specified in eq. (2.5) we are interested in taking their three-dimensional (3d) Fourier transforms, *i.e.* the (dimensionally regularized) functions

$$\bar{\mathcal{I}}_{\rm m}(x) \;\equiv\; \int_{\mathbf{p}} e^{i\mathbf{p}\cdot\mathbf{x}}\, \mathcal{I}_{\rm m}(p_n = 0, \mathbf{p}) \;. \tag{3.14}$$

We adopt a notation in the following whereby p stands for a four-vector with vanishing frequency, i.e. $p \equiv (0,\mathbf{p})$; in the above definitions, we can thus replace $P^2 \to p^2$, $(Q-P)^2 \to (p-Q)^2$, and $(R-P)^2 \to (p-R)^2$.

In some cases, the contribution of the zero modes ($q_n = r_n = 0$) to the master sum-integrals is delicate, and a proper handling requires the use of a consistent regularization procedure. We therefore separate the zero-mode contribution from the rest, and evaluate it in sec. 3.2; the results are denoted by $\bar{\mathcal{I}}^0_{\rm m}$. In subsequent sections, we assume that the zero modes have been subtracted from the sum-integrals; the subtracted sum-intergals are denoted by $\bar{\mathcal{I}}'_{\rm m}$.

3.2. Zero modes

Setting $q_n = r_n = 0$, we see that many of the master sum-integrals vanish as scaleless integrals in dimensional regularization,

$$\bar{\mathcal{J}}^0_{\rm a} \;=\; \bar{\mathcal{I}}^0_{\rm a} \;=\; \bar{\mathcal{I}}^0_{\rm b} \;=\; \bar{\mathcal{I}}^0_{\rm c} \;=\; \bar{\mathcal{I}}^0_{\rm d} \;=\; \bar{\mathcal{I}}^0_{\rm e} \;=\; 0 \;. \tag{3.15}$$

For the rest, we first note that by dimensional analysis,

$$\mathcal{J}^0_{\rm b} \sim T(p^2)^{\frac{3}{2}-\epsilon}\,, \tag{3.16}$$

$$\mathcal{I}^0_{\rm m} \sim T^2(p^2)^{1-2\epsilon}\,, \quad {\rm m}\in\{{\rm f,g,h,i,i',j}\}\,. \tag{3.17}$$

Recalling on the other hand that

$$\int_{\mathbf{p}} e^{i\mathbf{p}\cdot\mathbf{x}}\, p^{3-2\epsilon} = \frac{12}{\pi^2 x^6} + \mathcal{O}(\epsilon)\,, \quad \int_{\mathbf{p}} e^{i\mathbf{p}\cdot\mathbf{x}}\, p^{2-4\epsilon} = -\frac{6\epsilon}{\pi x^5} + \mathcal{O}(\epsilon^2)\,, \tag{3.18}$$

we observe that it suffices to evaluate the master integrals $\mathcal{I}^0_{\rm m}$ to order $1/\epsilon$. An elementary calculation (making use of the "zero-temperature parts" of the various master sum-integrals given in appendix A of ref. [12], after setting $D\to 3-2\epsilon$ in them) now produces

$$\bar{\mathcal{J}}^0_{\rm b} = \frac{96\pi^4 T^7}{\bar{x}^6} + \mathcal{O}(\epsilon), \tag{3.19}$$

$$\bar{\mathcal{I}}^0_{\rm f} = -\frac{3\pi^2 T^7}{\bar{x}^5} + \mathcal{O}(\epsilon), \tag{3.20}$$

$$\bar{\mathcal{I}}^0_{\rm g} = \mathcal{O}(\epsilon), \tag{3.21}$$

$$\bar{\mathcal{I}}^0_{\rm h} = \frac{3\pi^2 T^7}{\bar{x}^5} + \mathcal{O}(\epsilon), \tag{3.22}$$

$$\bar{\mathcal{I}}^0_{\rm i} = \frac{3\pi^2 T^7}{\bar{x}^5} + \mathcal{O}(\epsilon), \tag{3.23}$$

$$\bar{\mathcal{I}}^0_{\rm i'} = \mathcal{O}(\epsilon), \tag{3.24}$$

$$\bar{\mathcal{I}}^0_{\rm j} = \frac{6\pi^2 T^7}{\bar{x}^5} + \mathcal{O}(\epsilon)\,, \tag{3.25}$$

where we have defined the dimensionless variable

$$\bar{x} \equiv 2\pi T x\,, \tag{3.26}$$

in terms of which we will present our results.

3.3. $\bar{\mathcal{J}}_{\mathbf{a}}$ and $\bar{\mathcal{J}}_{\mathbf{b}}$

The 1-loop sum-integrals $\bar{\mathcal{J}}_{\rm a}$ and $\bar{\mathcal{J}}_{\rm b}$ are only needed in the combination

$$\begin{aligned}\bar{\mathcal{J}}_{\rm b} - 2\bar{\mathcal{J}}_{\rm a} &= \int_{\mathbf{p}} e^{i\mathbf{p}\cdot\mathbf{x}} p^2 \sum\!\!\!\!\!\!\int_Q \frac{1}{Q^2}\left\{\frac{p^2}{(p-Q)^2} - 2\right\} \\ &\to \int_{\mathbf{p}} e^{i\mathbf{p}\cdot\mathbf{x}} \sum\!\!\!\!\!\!\int_Q \frac{p^4}{Q^2(p-Q)^2}\,,\end{aligned} \tag{3.27}$$

where we have discarded a contact term. The remaining term can be evaluated in a straightforward manner by writing p^4 as a spatial derivative and using results derived in ref. [15]. We will later on also need the $\mathcal{O}(\epsilon)$ part but, for the time being, we merely write

$$\bar{\mathcal{J}}_{\rm b} - 2\bar{\mathcal{J}}_{\rm a} \;=\; \frac{4\pi^4 T^7}{\bar{x}} \frac{{\rm d}^4}{{\rm d}\bar{x}^4} \left(\frac{\coth\bar{x}}{\bar{x}} \right) + \mathcal{O}(\epsilon) \;. \tag{3.28}$$

Note that this expression contains both the zero-mode and the non-zero mode contributions; the zero-mode contribution of eq. (3.19) is recovered as the only power-law term at long distances, if we expand $\coth\bar{x} = 1 + \mathcal{O}(e^{-2\bar{x}})$.

3.4. $\bar{\mathcal{I}}_{\mathbf{a}}$, $\bar{\mathcal{I}}_{\mathbf{c}}$, $\bar{\mathcal{I}}_{\mathbf{e}}$

In momentum space, the P-dependence of the sum-integrals $\mathcal{I}_{\rm m}$, ${\rm m} \in \{{\rm a},{\rm c},{\rm e}\}$, factorizes from the Q and R dependences (in fact, $\mathcal{I}_{\rm e}$ vanishes identically). One is then left with taking a 3d Fourier transform of a non-negative integer power of the momentum squared, which leads to a result proportional to the delta function or its derivatives. The results could be directly extracted from ref. [12], but in the present paper we are only interested in finite values $\bar{x} \sim 1$, so we set these integrals to zero,

$$\bar{\mathcal{I}}_{\rm m} \to 0 \;, \quad {\rm m} \in \{{\rm a},{\rm c},{\rm e}\} \;. \tag{3.29}$$

Contact terms also appear as parts of the other master sum-integrals, and will be omitted there as well; again, if needed, they can be extracted from ref. [12].

3.5. $\bar{\mathcal{I}}_{\mathbf{b}}$, $\bar{\mathcal{I}}_{\mathbf{d}}$, $\bar{\mathcal{I}}_{\mathbf{g}}$

Next, consider the sum-integrals $\bar{\mathcal{I}}_{\rm m}$, ${\rm m} \in \{{\rm b},{\rm d},{\rm g}\}$. All of these consist of 1-loop integrals of the type that have been thoroughly investigated in the literature, see e.g. refs. [15]–[17]. Neglecting again contact terms, and noting that in eqs. (2.6), (2.7) the sum-integrals $\mathcal{I}_{\rm b}$ and $\mathcal{I}_{\rm g}$ are multiplied by terms of $\mathcal{O}(\epsilon)$, we obtain to the required order in ϵ:

$$\bar{\mathcal{I}}_{\rm b} \;=\; \mathcal{O}(\epsilon^0) \;, \tag{3.30}$$

$$\bar{\mathcal{I}}_{\rm d} \;=\; -\frac{\pi^2 T^7}{12} \frac{1}{\bar{x}} \frac{{\rm d}^3}{{\rm d}\bar{x}^3} \Big(\coth\bar{x} \Big) + \mathcal{O}(\epsilon) \;, \tag{3.31}$$

$$\bar{\mathcal{I}}_{\rm g} \;=\; \frac{\pi^2 T^7}{2} \frac{1}{\bar{x}} \frac{{\rm d}^4}{{\rm d}\bar{x}^4} \left(\frac{\coth\bar{x}}{\bar{x}} \right) \frac{1}{\epsilon} + \mathcal{O}(\epsilon^0) \;. \tag{3.32}$$

It is worth noting that the contribution of the zero mode $q_n = r_n = 0$ vanishes or is of $\mathcal{O}(\epsilon)$ in all of these cases, so it does not need to be separately subtracted.

3.6. $\bar{\mathcal{I}}'_{\mathbf{f}}$

As a warm-up for the more challenging integrals, let us consider $\bar{\mathcal{I}}'_{\rm f}$ in detail. Defining

$$\Pi(R) \;\equiv\; \sum\!\!\!\!\!\!\int_Q \frac{1}{Q^2(Q-R)^2} \;, \tag{3.33}$$

and using a representation from ref. [15] (cf. also eq. (3.41) below, with the flag α set to zero and the zero-mode part $T\delta_{r_n}/8r$ which has already been accounted for in eq. (3.20) omitted), we readily obtain for the sum-integral in question (the prime reminds of the zero-mode omission):

$$\begin{aligned}
\bar{\mathcal{I}}'_{\rm f} &= -\nabla^2 \int_{\mathbf{p}} e^{i\mathbf{p}\cdot\mathbf{x}} \biggl\{ \sum\!\!\!\!\!\!\int_R \frac{\Pi(R)}{(p-R)^2} \biggr\}' \\
&= -\nabla^2 \int_{\mathbf{p}} \sum\!\!\!\!\!\!\int_R \frac{e^{i(\mathbf{p}-\mathbf{r})\cdot\mathbf{x}}}{(p-R)^2} \biggl[\frac{e^{i\mathbf{r}\cdot\mathbf{x}}}{(4\pi)^2} \left(\frac{\bar{\Lambda}^2}{R^2}\right)^{\epsilon} \left(\frac{1}{\epsilon}+2\right) \\
&\qquad\qquad + \frac{T}{(4\pi)^2} \int \mathrm{d}^3\mathbf{y}\, \frac{e^{i\mathbf{r}\cdot(\mathbf{x}+\mathbf{y})}}{y^2} \left(\coth\bar{y} - \frac{1}{\bar{y}} - \delta_{r_n} \right) e^{-|r_n|y} \biggr] \\
&= -\frac{T\nabla^2}{(4\pi)^3} \biggl[\bar{\Lambda}^{2\epsilon} \left(\frac{1}{\epsilon}+2\right) \sum_{r_n} \frac{e^{-|r_n|x}}{x} \int_{\mathbf{r}} e^{i\mathbf{r}\cdot\mathbf{x}} \frac{1}{(R^2)^{\epsilon}} \\
&\qquad\qquad + T \sum_{r_n} \frac{e^{-2|r_n|x}}{x^3} \left(\coth\bar{x} - \frac{1}{\bar{x}} - \delta_{r_n} \right) \biggr] \\
&= -\frac{3\pi^2 T^7}{4} \frac{1}{\bar{x}} \frac{\mathrm{d}^2}{\mathrm{d}\bar{x}^2} \left(\frac{1}{\bar{x}^2 \sinh^2\bar{x}} \right) + \mathcal{O}(\epsilon) \;.
\end{aligned} \tag{3.34}$$

In the last step we expanded in ϵ and dropped contact terms; we also inserted the integrals

$$\int_{\mathbf{r}} \frac{e^{i\mathbf{r}\cdot\mathbf{x}}}{r_n^2+r^2} = \frac{e^{-|r_n|x}}{4\pi x} \;, \quad \int_{\mathbf{r}} e^{i\mathbf{r}\cdot\mathbf{x}} \ln(r_n^2+r^2) = -\frac{1}{2\pi x^3}(1+|r_n|x)e^{-|r_n|x} \;, \tag{3.35}$$

and carried out subsequently the elementary sums over r_n,

$$\sum_{r_n} e^{-2|r_n|x} = \coth\bar{x} \;, \quad \sum_{r_n} |r_n| x\, e^{-2|r_n|x} = \frac{\bar{x}}{2\sinh^2\bar{x}} \;. \tag{3.36}$$

3.7. $\bar{\mathcal{I}}'_{\mathbf{h}}$

Next, we inspect the sum-integral $\bar{\mathcal{I}}'_{\rm h}$, the evaluation of which is in many ways similar to that of $\bar{\mathcal{I}}'_{\rm f}$. Separating again the zero temperature part of $\Pi(R)$ from the rest, we obtain

$$\begin{aligned}
\bar{\mathcal{I}}'_{\rm h} &= \frac{\bar{\Lambda}^{2\epsilon}}{(4\pi)^2} \left(\frac{1}{\epsilon}+2\right) \int_{\mathbf{p}} e^{i\mathbf{p}\cdot\mathbf{x}} \sum\!\!\!\!\!\!\int_R \frac{p^4}{(R^2)^{1+\epsilon}(p-R)^2} \\
&\quad + \frac{T}{(4\pi)^2} \nabla^4 \int_{\mathbf{p}} e^{i\mathbf{p}\cdot\mathbf{x}} \sum\!\!\!\!\!\!\int_R \frac{1}{R^2(p-R)^2} \int \mathrm{d}^3\mathbf{y}\, \frac{e^{i\mathbf{r}\cdot\mathbf{y}}}{y^2} \left(\coth\bar{y} - \frac{1}{\bar{y}} - \delta_{r_n} \right) e^{-|r_n|y} \\
&\equiv \bar{\mathcal{I}}^0_{\rm h} + \bar{\mathcal{I}}^T_{\rm h} \;,
\end{aligned} \tag{3.37}$$

where we leave the first part intact for now (we return to it in sec. 3.11) and only consider the second term, $\bar{\mathcal{I}}^T_{\rm h}$. For this function, we obtain

$$\begin{aligned}\bar{\mathcal{I}}^T_{\rm h} &= \frac{T^2\nabla^4}{(4\pi)^4}\left[\frac{1}{x}\sum_{r_n}\int {\rm d}^3\mathbf{y}\,\frac{1}{y^2|\mathbf{x}-\mathbf{y}|}\left(\coth\bar{y}-\frac{1}{\bar{y}}-\delta_{r_n}\right)e^{-|r_n|(x+y+|\mathbf{x}-\mathbf{y}|)}\right]\\ &= -\frac{\pi^2T^7}{2\bar{x}}\,\frac{{\rm d}^4}{{\rm d}\bar{x}^4}\int_0^\infty\frac{{\rm d}\bar{y}}{\bar{x}\bar{y}}\left\{\left(\coth\bar{y}-\frac{1}{\bar{y}}\right)\left[\bar{y}_<+\ln\left(\frac{e^{2\bar{y}_>}-1}{e^{2(\bar{x}+\bar{y})}-1}\right)\right]+\bar{y}_<\right\}, \quad (3.38)\end{aligned}$$

where $\bar{y}_< \equiv \min(\bar{y},\bar{x})$ and $\bar{y}_> \equiv \max(\bar{y},\bar{x})$. After taking the derivatives with respect to $\bar{x}$, we are left with an integral that appears to be difficult to perform analytically, but is numerically quite benign. Thus, we have opted to evaluate it numerically (cf. sec. 4).

3.8. $\bar{\mathcal{I}}'_{\rm i}$

As in ref. [12], we reduce the evaluation of $\bar{\mathcal{I}}'_{\rm i}$ to the other integrals, in particular $\bar{\mathcal{I}}'_{\rm i'}$, employing the relation

$$\bar{\mathcal{I}}'_{\rm i} = \bar{\mathcal{I}}'_{\rm a} + \bar{\mathcal{I}}'_{\rm e} - \bar{\mathcal{I}}'_{\rm f} + \bar{\mathcal{I}}'_{\rm i'}\,. \quad (3.39)$$

3.9. $\bar{\mathcal{I}}'_{\rm i'}$

The evaluation of $\bar{\mathcal{I}}'_{\rm i'}$ involves a new type of 1-loop "self-energy" structure, as instead of $\Pi(R)$ of eq. (3.33) it contains the function

$$\Pi_{ij}(R) \equiv \sum\!\!\!\!\!\!\int_Q \frac{q_iq_j}{Q^2(Q-R)^2} = A(R)\,\delta_{ij} + B(R)\,r_ir_j\,, \quad (3.40)$$

where in the latter step we have used three-dimensional rotational symmetry to write the tensor in terms of two scalar quantities. As usual A and B can be determined by projecting the defining equation with δ_{ij} and r_ir_j; moreover, by completing squares, the results can be reduced to the known tadpole $\sum\!\!\!\!\!\!\int_Q 1/Q^2 = T^2/12$ as well as to the self-energies (cf. refs. [15, 17])

$$\begin{aligned}\sum\!\!\!\!\!\!\int_Q \frac{1}{Q^2(Q-R)^2} &= \frac{1}{(4\pi)^2}\left(\frac{\bar{\Lambda}^2}{R^2}\right)^\epsilon\left(\frac{1}{\epsilon}+2\right)+\frac{\alpha\,T^2}{6R^2}+\frac{T\delta_{r_n}}{8r}\\ &\quad+\frac{T}{(4\pi)^2}\int{\rm d}^3\mathbf{y}\,\frac{e^{i\mathbf{r}\cdot\mathbf{y}}}{y^2}\left(\coth\bar{y}-\frac{1}{\bar{y}}-\frac{\alpha\,\bar{y}}{3}-\delta_{r_n}\right)e^{-|r_n|y}\,, \quad (3.41)\\ \sum\!\!\!\!\!\!\int_Q \frac{4q_n^2-r_n^2}{Q^2(Q-R)^2} &= -\frac{1}{(4\pi)^2}\left(\frac{\bar{\Lambda}^2}{R^2}\right)^\epsilon\frac{r^2}{D-1}\left(\frac{1}{\epsilon}+2\right)+\frac{\alpha\,T^2r_n^2}{6R^2}\\ &\quad+\frac{T}{(4\pi)^2}\int{\rm d}^3\mathbf{y}\,\frac{e^{i\mathbf{r}\cdot\mathbf{y}}}{y^2}\partial_y^2\left[\left(\coth\bar{y}-\frac{1}{\bar{y}}-\frac{\alpha\,\bar{y}}{3}-\delta_{r_n}\right)e^{-|r_n|y}\right]. \quad (3.42)\end{aligned}$$

The coefficient α serves as a "flag", to be chosen freely (below $\alpha = 1$ for $r_n \neq 0$). Note that in eq. (3.42) the zero-mode subtraction has actually no influence; $\partial_y^2[\,1\,] = 0$.

Defining now, for brevity,

$$f_n(y) \equiv \left(\coth\bar{y} - \frac{1}{\bar{y}} - \frac{\bar{y}}{3} - \delta_{r_n}\right)e^{-|r_n|y} , \tag{3.43}$$

$$\tilde{f}_n(y) \equiv \left(\coth\bar{y} - \frac{1}{\bar{y}} - \frac{\bar{y}}{3} - \left(1-\frac{\bar{y}}{3}\right)\delta_{r_n}\right)e^{-|r_n|y} , \tag{3.44}$$

where in the latter case we have, for future convenience, removed the α-flagged contribution in the case of the zero-mode, the functions A and B become

$$\begin{aligned} A(R) &= -\frac{R^2}{4(D-1)}\frac{1}{(4\pi)^2}\left(\frac{\bar{\Lambda}^2}{R^2}\right)^{\epsilon}\left(\frac{1}{\epsilon}+2\right) - \left\{\frac{Tr}{64}\delta_{r_n}\right\} \\ &\quad - \frac{R^2}{8r^2}\frac{T}{(4\pi)^2}\int \mathrm{d}^3\mathbf{y}\,\frac{e^{i\mathbf{r}\cdot\mathbf{y}}}{y^2}(\partial_y^2 + r^2)f_n(y) , \end{aligned} \tag{3.45}$$

$$\begin{aligned} B(R) &= \frac{D}{4(D-1)}\frac{1}{(4\pi)^2}\left(\frac{\bar{\Lambda}^2}{R^2}\right)^{\epsilon}\left(\frac{1}{\epsilon}+2\right) + \left(\frac{1}{12} - \frac{\delta_{r_n}}{16}\right)\frac{T^2}{R^2} + \left\{\frac{3T}{64r}\delta_{r_n}\right\} \\ &\quad + \frac{1}{8r^4}\frac{T}{(4\pi)^2}\int \mathrm{d}^3\mathbf{y}\,\frac{e^{i\mathbf{r}\cdot\mathbf{y}}}{y^2}\Big[(3R^2-2r^2)\partial_y^2 + (R^2+2r^2)r^2\Big]\tilde{f}_n(y) . \end{aligned} \tag{3.46}$$

Defining $A' \equiv A + \{\frac{Tr}{64}\delta_{r_n}\}$ and $B' \equiv B - \{\frac{3T}{64r}\delta_{r_n}\}$, i.e. dropping the terms whose effects were already accounted for in eq. (3.24), the sum-integral under study becomes

$$\begin{aligned} \bar{\mathcal{I}}'_{\mathrm{i}'} &= 4\int_{\mathbf{p}} e^{i\mathbf{p}\cdot\mathbf{x}} \sum\!\!\!\!\!\!\int_R \frac{1}{R^2(p-R)^2}\Big[p^2A'(R) + (\mathbf{p}\cdot\mathbf{r})^2B'(R)\Big] \\ &= -4\nabla^2 T\sum_{r_n}\frac{e^{-|r_n|x}}{4\pi x}\int_{\mathbf{r}} e^{i\mathbf{r}\cdot\mathbf{x}}\frac{A'(R)}{R^2} + 4T\sum_{r_n}\int_{\mathbf{p}}\frac{e^{i\mathbf{p}\cdot\mathbf{x}}}{p^2+r_n^2}\int_{\mathbf{r}}\frac{e^{i\mathbf{r}\cdot\mathbf{x}}}{R^2}(r^2+\mathbf{p}\cdot\mathbf{r})^2B'(R) \\ &= 4T\sum_{r_n}\left\{-\nabla^2\left(\frac{e^{-|r_n|x}}{4\pi x}\int_{\mathbf{r}} e^{i\mathbf{r}\cdot\mathbf{x}}\frac{A'(R)}{R^2}\right) + \frac{\partial^2}{\partial x_i\partial x_j}\left[\frac{e^{-|r_n|x}}{4\pi x}\frac{\partial^2}{\partial x_i\partial x_j}\int_{\mathbf{r}} e^{i\mathbf{r}\cdot\mathbf{x}}\frac{B'(R)}{R^2}\right]\right\} \\ &\equiv 4\left(\bar{\mathcal{I}}^A_{\mathrm{i}'} + \bar{\mathcal{I}}^B_{\mathrm{i}'}\right) , \end{aligned} \tag{3.47}$$

which defines the two functions we now set out to compute.

Let us start with $\bar{\mathcal{I}}^A_{\mathrm{i}'}$ and divide it into two parts according to the two terms in eq. (3.45),

$$\bar{\mathcal{I}}^A_{\mathrm{i}'} \equiv \bar{\mathcal{I}}^{A0}_{\mathrm{i}'} + \bar{\mathcal{I}}^{AT}_{\mathrm{i}'} , \tag{3.48}$$

where the first "zero-temperature" piece reads

$$\begin{aligned} \bar{\mathcal{I}}^{A0}_{\mathrm{i}'} &= \frac{1}{4(D-1)}\frac{\bar{\Lambda}^{2\epsilon}}{(4\pi)^3}\left(\frac{1}{\epsilon}+2\right)T\sum_{r_n}\nabla^2\left[\frac{e^{-|r_n|x}}{x}\int_{\mathbf{r}}\frac{e^{i\mathbf{r}\cdot\mathbf{x}}}{(R^2)^{\epsilon}}\right] \\ &= \frac{T}{6(4\pi)^4}\nabla^2\left[\frac{1}{x^4}\sum_{r_n}(1+|r_n|x)\,e^{-2|r_n|x}\right] \\ &= -\frac{\pi^2T^7}{48}\frac{1}{\bar{x}}\frac{\mathrm{d}^3}{\mathrm{d}\bar{x}^3}\left(\frac{\coth\bar{x}}{\bar{x}^2}\right) . \end{aligned} \tag{3.49}$$

In the second step we expanded in ϵ, dropped contact terms, and made use of eq. (3.35); in the last step the sums were carried out like in eq. (3.36). The finite temperature part can, on the other hand, be written as

$$\begin{aligned}
\bar{\mathcal{I}}_{\mathrm{i}'}^{AT} &= \frac{T^2}{8(4\pi)^3}\nabla^2 \sum_{r_n} \frac{e^{-|r_n|x}}{x} \int \frac{\mathrm{d}^3\mathbf{y}}{y^2} \int_{\mathbf{r}} e^{i\mathbf{r}\cdot(\mathbf{x}+\mathbf{y})} \left(1 + \frac{1}{r^2}\partial_y^2\right) f_n(y) \\
&= \frac{T^2}{8(4\pi)^3}\nabla^2 \sum_{r_n} \frac{e^{-|r_n|x}}{x} \left[\frac{f_n(x)}{x^2} + \int \mathrm{d}^3\mathbf{y}\, \frac{1}{4\pi y^2|\mathbf{x}+\mathbf{y}|}\partial_y^2 f_n(y)\right] \\
&= \frac{T^2}{8(4\pi)^3}\nabla^2 \sum_{r_n} \frac{e^{-|r_n|x}}{x} \left[\frac{f_n(x)}{x^2} + \int_0^\infty \mathrm{d}y\, \frac{1}{y_>}\partial_y^2 f_n(y)\right] \\
&= \frac{T^2}{4(4\pi)^3}\nabla^2 \sum_{r_n} \frac{e^{-|r_n|x}}{x} \int_x^\infty \mathrm{d}y\, \frac{f_n(y)}{y^3} \\
&= \frac{\pi^2 T^7}{8\bar{x}} \frac{\mathrm{d}^2}{\mathrm{d}\bar{x}^2} \int_{\bar{x}}^\infty \frac{\mathrm{d}\bar{y}}{\bar{y}^3} \left[\coth\left(\frac{\bar{x}+\bar{y}}{2}\right)\left(\coth\bar{y} - \frac{1}{\bar{y}} - \frac{\bar{y}}{3}\right) - 1\right], \qquad (3.50)
\end{aligned}$$

where the last integral again seems to require numerical evaluation.

Moving then on to $\bar{\mathcal{I}}_{\mathrm{i}'}^{B}$, we once more split the integral into two parts, now according to the $T = 0$ and $T \neq 0$ terms of $B'(Q)$. This produces

$$\begin{aligned}
\bar{\mathcal{I}}_{\mathrm{i}'}^{B} &\equiv \bar{\mathcal{I}}_{\mathrm{i}'}^{B0} + \bar{\mathcal{I}}_{\mathrm{i}'}^{BT}, \\
\bar{\mathcal{I}}_{\mathrm{i}'}^{B0} &= \frac{D}{4(D-1)} \frac{\bar{\Lambda}^{2\epsilon}}{(4\pi)^2} \left(\frac{1}{\epsilon} + 2\right) \int_{\mathbf{p}} e^{i\mathbf{p}\cdot\mathbf{x}} \sum\!\!\!\!\!\!\int_R \frac{(\mathbf{p}\cdot\mathbf{r})^2}{(R^2)^{1+\epsilon}(p-R)^2}, \qquad (3.51)
\end{aligned}$$

which we analyse together with the other divergent terms in sec. 3.11. With $\bar{\mathcal{I}}_{\mathrm{i}'}^{BT}$, on the other hand, we encounter a similar albeit more complicated expression as with $\bar{\mathcal{I}}_{\mathrm{i}'}^{AT}$. Its evaluation nevertheless proceeds along the same lines: One begins by performing the spatial $\mathbf{r}$ integral, then takes care of the angular part of the $\mathbf{y}$ integration, partially integrates, and finally performs the sum over r_n (which we leave intact for the moment). The result of the procedure reads (a prime indicating the omission of the zero-mode)

$$\begin{aligned}
\bar{\mathcal{I}}_{\mathrm{i}'}^{BT} &= \frac{T}{4\pi}{\sum_{r_n}}' \frac{\partial^2}{\partial x_i \partial x_j} \frac{e^{-|r_n|x}}{x} \frac{\partial^2}{\partial x_i \partial x_j} \left\{ \frac{T^2}{12} \frac{e^{-|r_n|x}}{8\pi|r_n|} \right. \\
&\quad - \frac{T}{8(4\pi)^2} \frac{2}{|r_n^3|x} \int_0^\infty \frac{\mathrm{d}y}{y^3} \left(1 + |r_n|y + r_n^2 y^2\right) e^{-|r_n|(x+y)} f_n(y) \\
&\quad + \frac{T}{8(4\pi)^2} \frac{2}{|r_n^3|x} \int_0^x \frac{\mathrm{d}y}{y^3} \left(1 - |r_n|y + r_n^2 y^2\right) e^{-|r_n|(x-y)} f_n(y) \\
&\quad \left. + \frac{T}{8(4\pi)^2} \int_x^\infty \frac{\mathrm{d}y}{y^3} \left[y^2 - x^2 - \frac{4}{r_n^2} + \frac{2}{|r_n^3|x} \left(1 + |r_n|y + r_n^2 y^2\right) e^{-|r_n|(y-x)}\right] f_n(y) \right\} \\
&+ \frac{T^2}{8(4\pi)^3} \frac{\partial^2}{\partial x_i \partial x_j} \frac{1}{x} \frac{\partial^2}{\partial x_i \partial x_j} \left\{ \frac{8}{3x} \int_0^x \mathrm{d}y\, \tilde{f}_0(y) + \int_x^\infty \mathrm{d}y \left(\frac{3}{y} - \frac{x^2}{3y^3}\right) \tilde{f}_0(y) \right\}. \qquad (3.52)
\end{aligned}$$

The derivatives can be taken by noting that the independence of the above expressions on angular variables implies

$$\partial_i\partial_j\Big[g(x)\partial_i\partial_j f(x)\Big] \;=\; \frac{1}{x^2}\partial_x^2\left(x^2 g f''\right) - \frac{2}{x^2}\partial_x\left(g f'\right)\;. \tag{3.53}$$

Then the first row can be simplified into

$$\begin{aligned}
&\frac{T}{4\pi}{\sum_{r_n}}' \frac{\partial^2}{\partial x_i\partial x_j}\left\{\frac{e^{-|r_n|x}}{x}\frac{\partial^2}{\partial x_i\partial x_j}\left[\frac{T^2}{12}\frac{e^{-|r_n|x}}{8\pi|r_n|}\right]\right\} \\
&\quad= \frac{\pi^2T^7}{3}\left[-\frac{n(2\bar{x})}{2\bar{x}^4}+\frac{n'(2\bar{x})}{\bar{x}^3}-\frac{n''(2\bar{x})}{\bar{x}^2}-\frac{n^{(3)}(2\bar{x})}{\bar{x}}\right],
\end{aligned} \tag{3.54}$$

where n stands for the bosonic distribution function $n(x)\equiv 1/(e^x-1)$, whereas the last row (the contribution from $r_n=0$, $q_n\neq 0$) becomes

$$\begin{aligned}
&\frac{T^2}{8(4\pi)^2}\frac{\partial^2}{\partial x_i\partial x_j}\left\{\frac{1}{4\pi x}\frac{\partial^2}{\partial x_i\partial x_j}\left[\frac{8}{3x}\int_0^x \mathrm{d}y\,\tilde{f}_0(y)+\int_x^\infty \mathrm{d}y\,\left(\frac{3}{y}-\frac{x^2}{3y^3}\right)\tilde{f}_0(y)\right]\right\} \\
&\quad= \frac{\pi^2T^7}{4}\left[\frac{9}{\bar{x}^6}+\frac{4}{\bar{x}^6}\ln\left(\frac{1-e^{-2\bar{x}}}{2\bar{x}}\right)-\frac{11\,n(2\bar{x})}{\bar{x}^5}+\frac{10\,n'(2\bar{x})}{\bar{x}^4}-\frac{4\,n''(2\bar{x})}{\bar{x}^3}\right].
\end{aligned} \tag{3.55}$$

The other parts contain integrals that we collect together in sec. 4 for numerical evaluation.

3.10. $\bar{\mathcal{I}}'_{\mathrm{j}}$

From the numerics point of view, the sum-integral $\bar{\mathcal{I}}'_{\mathrm{j}}$ appears to be the most non-trivial one, as there are not many analytic tricks that we can apply to it. The most important observation is that $\bar{\mathcal{I}}'_{\mathrm{j}}$ is both UV and IR finite, implying that we can set $\epsilon=0$ and consider its evaluation in three-dimensional coordinate space. Fourier transforming all the propagators and subsequently rescaling the radial coordinates by x, we obtain

$$\begin{aligned}
\bar{\mathcal{I}}'_{\mathrm{j}} &= -\frac{T^2\nabla^6}{(4\pi)^5}\int \mathrm{d}^3\mathbf{y}\,\mathrm{d}^3\mathbf{z}\,\frac{{\sum_{q_n,r_n}}' e^{-|q_n|(y+z)-|r_n|(|\mathbf{x}-\mathbf{y}|+|\mathbf{x}-\mathbf{z}|)-|q_n-r_n||\mathbf{y}-\mathbf{z}|}}{yz|\mathbf{x}-\mathbf{y}||\mathbf{x}-\mathbf{z}||\mathbf{y}-\mathbf{z}|} \\
&= -\frac{\pi T^7}{16\bar{x}}\int_0^\infty \mathrm{d}\tilde{y}\,\mathrm{d}\tilde{z}\int_{-1}^1 \mathrm{d}t_1\,\mathrm{d}t_2\int_0^{2\pi}\mathrm{d}\phi\,\frac{\tilde{y}\tilde{z}}{|\mathbf{e}-\tilde{\mathbf{y}}||\mathbf{e}-\tilde{\mathbf{z}}||\tilde{\mathbf{y}}-\tilde{\mathbf{z}}|} \\
&\qquad\times\frac{\mathrm{d}^6}{\mathrm{d}\bar{x}^6}\left\{\bar{x}^2{\sum_{m,n}}' e^{-\bar{x}\left[|m|(\tilde{y}+\tilde{z})+|n|(|\mathbf{e}-\tilde{\mathbf{y}}|+|\mathbf{e}-\tilde{\mathbf{z}}|)+|m-n||\tilde{\mathbf{y}}-\tilde{\mathbf{z}}|\right]}\right\},
\end{aligned} \tag{3.56}$$

where $\mathbf{e}$ is a unit vector and the prime on the sum means that the simultaneous zero mode $m=n=0$ has been left out. This sum can now be explicitly carried out, giving

$$\begin{aligned}
\bar{\mathcal{I}}'_{\mathrm{j}} &= -\frac{\pi T^7}{8\bar{x}}\int_0^\infty \mathrm{d}\tilde{y}\,\mathrm{d}\tilde{z}\int_{-1}^1 \mathrm{d}t_1\,\mathrm{d}t_2\int_0^{2\pi}\mathrm{d}\phi\,\frac{\tilde{y}\tilde{z}}{|\mathbf{e}-\tilde{\mathbf{y}}||\mathbf{e}-\tilde{\mathbf{z}}||\tilde{\mathbf{y}}-\tilde{\mathbf{z}}|} \\
&\quad\times\frac{\mathrm{d}^6}{\mathrm{d}\bar{x}^6}\left\{\bar{x}^2\Big[n(\bar{x}a)+n(\bar{x}b)+n(\bar{x}c)+n(\bar{x}a)n(\bar{x}b)+n(\bar{x}b)n(\bar{x}c)+n(\bar{x}c)n(\bar{x}a)\Big]\right\},
\end{aligned} \tag{3.57}$$

where we have defined the combinations $a \equiv \tilde{y} + \tilde{z} + |\mathbf{e} - \tilde{\mathbf{y}}| + |\mathbf{e} - \tilde{\mathbf{z}}|$, $b \equiv \tilde{y} + \tilde{z} + |\tilde{\mathbf{y}} - \tilde{\mathbf{z}}|$ and $c \equiv |\mathbf{e} - \tilde{\mathbf{y}}| + |\mathbf{e} - \tilde{\mathbf{z}}| + |\tilde{\mathbf{y}} - \tilde{\mathbf{z}}|$. The sixth derivative of the expression on the last line contains a large number of terms, but its evaluation is straightforward to automatize using the relation $n'(x) = -n(x)[1 + n(x)]$. The remaining 5d integral can be performed using numerical methods.

3.11. Divergent terms

Above, we have left two integrals unevaluated, namely the UV-divergent term $\bar{\mathcal{I}}^0_{\rm h}$ of eq. (3.37) and $\bar{\mathcal{I}}^{B0}_{\rm i'}$ of eq. (3.51). These contributions are expected to partially cancel against the renormalization of the gauge coupling in connection with the 1-loop terms in eqs. (2.6) and (2.7). Here, we evaluate the sum of these three functions, obtaining a UV-finite result.

Inspecting the forms of $\bar{G}_\theta(x)$ and $\bar{G}_\chi(x)$ in eqs. (2.6) and (2.7), we observe that the only parts containing divergences are

$$\frac{\bar{G}^{\rm div}_\theta}{4d_A c^2_\theta} = \frac{\bar{G}^{\rm div}_\chi}{-16 d_A c^2_\chi (D-3)} = (D-2)\left[\frac{g^4_{\rm B}}{2}\bar{\mathcal{J}}_{\rm b} + g^6_{\rm B} N_{\rm c}\Big(3\bar{\mathcal{I}}^0_{\rm h} + 2\times 4\bar{\mathcal{I}}^{B0}_{\rm i'}\Big)\right] . \tag{3.58}$$

Expanding $g^2_{\rm B}$ according to eq. (2.2), we are left to consider the combination

$$\begin{aligned}
\bar{\mathcal{I}}_{\rm div} &\equiv -\frac{1}{(4\pi)^2}\,\frac{11}{3\epsilon}\,\bar{\mathcal{J}}_b + 3\bar{\mathcal{I}}^0_{\rm h} + 8\bar{\mathcal{I}}^{B0}_{\rm i'} \\
&= \frac{1}{(4\pi)^2}\int_{\mathbf{p}} e^{i\mathbf{p}\cdot\mathbf{x}} \sum\!\!\!\!\!\!\int_R \frac{1}{R^2(p-R)^2}\bigg\{ -\frac{11p^4}{3\epsilon} \\
&\qquad + \left(\frac{1}{\epsilon}+2\right)\left(\frac{\bar{\Lambda}^2}{R^2}\right)^{\epsilon}\left(3p^4 + \frac{2D}{D-1}\,(\mathbf{p}\cdot\mathbf{r})^2\right)\bigg\} \\
&= \frac{2}{3(4\pi)^2}\int_{\mathbf{p}} e^{i\mathbf{p}\cdot\mathbf{x}} \sum\!\!\!\!\!\!\int_R \frac{1}{R^2(p-R)^2}\bigg\{ \frac{4(\mathbf{p}\cdot\mathbf{r})^2 - p^4}{\epsilon} \\
&\qquad + 9p^4 + \frac{26(\mathbf{p}\cdot\mathbf{r})^2}{3} + \left(\frac{9p^4}{2} + 4(\mathbf{p}\cdot\mathbf{r})^2\right)\ln\frac{\bar{\Lambda}^2}{R^2}\bigg\} .
\end{aligned} \tag{3.59}$$

Writing the scalar products $(\mathbf{p}\cdot\mathbf{r})^2$ in terms of $(p-R)^2$, we can massage the result into a relatively simple form; in particular, apart from contact terms, the $1/\epsilon$ divergence disappears in the course of the $\mathbf{r}$-integration. Upon denoting

$$D_a(x, r_n) \equiv \int \frac{{\rm d}^3\mathbf{r}}{(2\pi)^3}\, e^{i\mathbf{r}\cdot\mathbf{x}} \frac{1}{(R^2)^a} , \tag{3.60}$$

$$\widetilde{D}_a(x, r_n) \equiv \int \frac{{\rm d}^3\mathbf{r}}{(2\pi)^3}\, e^{i\mathbf{r}\cdot\mathbf{x}} \frac{\ln(\bar{\Lambda}^2/R^2)}{(R^2)^a} , \tag{3.61}$$

the remaining finite result becomes

$$\bar{\mathcal{I}}_{\rm div} = \frac{2T}{3(4\pi)^2}\sum_{r_n}\Big\{\nabla^4\Big[D_1(x,r_n)\Big(\frac{67}{6}\,D_1(x,r_n)+\frac{11}{2}\,\widetilde{D}_1(x,r_n)\Big)\Big] - 2\nabla^2\Big[D_1(x,r_n)\widetilde{D}_0(x,r_n)\Big]+D_1(x,r_n)\widetilde{D}_{-1}(x,r_n)\Big\}\,. \quad (3.62)$$

The various functions that appear here have the forms

$$D_1(x,r_n) = \frac{e^{-|r_n|x}}{4\pi x}\,, \quad (3.63)$$

$$\widetilde{D}_1(x,r_n) = \frac{e^{-|r_n|x}}{4\pi x}\left[2\ln\left(e^{\gamma_{\rm E}}\bar{\Lambda}x\right)+|r_n|x\int_0^\infty {\rm d}\tilde{y}\,e^{-\tilde{y}|r_n|x}\ln\Big(\frac{\tilde{y}}{2+\tilde{y}}\Big)\right], \quad (3.64)$$

$$\widetilde{D}_0(x,r_n) = \frac{(1+|r_n|x)e^{-|r_n|x}}{2\pi x^3}\,, \quad (3.65)$$

$$\widetilde{D}_{-1}(x,r_n) = -\frac{(3+3|r_n|x+r_n^2x^2)e^{-|r_n|x}}{\pi x^5}\,, \quad (3.66)$$

which at the end leads to the result

$$\bar{\mathcal{I}}_{\rm div} = \pi^2T^7\Big\{\frac{44\ln\left(e^{\gamma_{\rm E}}\bar{\Lambda}x\right)-57}{\bar{x}^6}-\frac{1}{3\bar{x}}\frac{{\rm d}^2}{{\rm d}\bar{x}^2}\Big[\frac{n(2\bar{x})}{\bar{x}^3}\Big]+\frac{2}{3\bar{x}}\frac{{\rm d}^3}{{\rm d}\bar{x}^3}\Big[\frac{n(2\bar{x})}{\bar{x}^2}\Big] + \frac{1}{\bar{x}}\frac{{\rm d}^4}{{\rm d}\bar{x}^4}\Big[\frac{67+66\ln\left(e^{\gamma_{\rm E}}\bar{\Lambda}x\right)}{18\bar{x}(e^{2\bar{x}}-1)}+\frac{33}{18}\int_0^\infty {\rm d}\tilde{y}\,\ln\Big(\frac{2+\tilde{y}}{\tilde{y}}\Big)n'\Big((2+\tilde{y})\bar{x}\Big)\Big]\Big\}\,. \quad (3.67)$$

4. Basic results

4.1. General expressions

We are now ready to write down our final results for the full theory contributions to the correlators $\bar{G}_\theta^{\rm F}(x)$ and $\bar{G}_\chi^{\rm F}(x)$, from eqs. (2.6), (2.7) and (3.39). Omitting contact terms and collecting terms up to $\mathcal{O}(\epsilon^0)$, we obtain

$$\frac{\bar{G}_\theta^{\rm F}}{4d_A c_\theta^2} = g^4\bar{\mathcal{J}}_{\rm b} + 2g^6 N_{\rm c}\Big[\bar{\mathcal{I}}_{\rm div} - 2\bar{\mathcal{I}}_{\rm d} - 3\bar{\mathcal{I}}_{\rm f} + 3\bar{\mathcal{I}}_{\rm h} + 2\bar{\mathcal{I}}_{\rm i'} - \bar{\mathcal{I}}_{\rm j}\Big] \,, \tag{4.1}$$

$$\frac{\bar{G}_\chi^{\rm F}}{-16d_A c_\chi^2} = g^4\bar{\mathcal{J}}_{\rm b} + 2g^6 N_{\rm c}\Big[\bar{\mathcal{I}}_{\rm div} - 2\bar{\mathcal{I}}_{\rm d} - 3\bar{\mathcal{I}}_{\rm f} + 3\bar{\mathcal{I}}_{\rm h} + 2\bar{\mathcal{I}}_{\rm i'} - \bar{\mathcal{I}}_{\rm j} + 2\epsilon\bar{\mathcal{I}}_{\rm g}\Big] \,. \tag{4.2}$$

It is immediately clear that the two channels only differ through a single term, the last one in eq. (4.2). Inserting the result from eq. (3.32), the difference has a simple form; it is shown explicitly in eqs. (4.6), (4.7) below and is displayed numerically in fig. 2.

Adding up the various parts from sec. 3 and defining the functions

$$n(x) = \frac{1}{e^x-1} = \sum_{n=1}^{\infty} e^{-nx} \,, \qquad i(x) \equiv \ln(1-e^{-x}) = -\sum_{n=1}^{\infty}\frac{e^{-nx}}{n} \,, \tag{4.3}$$

$$\mathrm{Li}_2(e^{-x}) \equiv \sum_{n=1}^{\infty}\frac{e^{-nx}}{n^2} \,, \qquad \mathrm{Li}_3(e^{-x}) \equiv \sum_{n=1}^{\infty}\frac{e^{-nx}}{n^3} \,, \tag{4.4}$$

we end up with the expressions

$$\begin{aligned}\frac{\bar{G}_\theta^{\rm F}(x)}{4d_A c_\theta^2} &= g^4\, 4\pi^4 T^7\, \phi_{\rm LO}(\bar{x}) \\ &+ g^6 N_{\rm c}\,\pi^2 T^7\left\{\frac{11}{3}\,\phi_{\rm LO}(\bar{x})\,\ln\left(\frac{e^{\gamma_{\rm E}}\bar{\Lambda}\bar{x}}{2\pi T}\right) + \phi_{\rm NLO}(\bar{x}) + \phi_1(\bar{x}) + \phi_2(\bar{x})\right\} \,, \end{aligned} \tag{4.5}$$

$$\frac{\bar{G}_\chi^{\rm F}(x)}{-16d_A c_\chi^2} = \frac{\bar{G}_\theta^{\rm F}(x)}{4d_A c_\theta^2} + g^6 N_{\rm c}\, 2\pi^2 T^7\,\phi_{\rm LO}(\bar{x}) \,. \tag{4.6}$$

The function $\phi_{\rm LO}$, which determines the leading-order behaviour, the scale dependence, as well as the difference between the two channels, is given by (cf. eq. (3.28))

$$\phi_{\rm LO}(\bar{x}) = \frac{24}{\bar{x}^6} + \frac{2}{\bar{x}}\frac{{\rm d}^4}{{\rm d}\bar{x}^4}\left(\frac{n(2\bar{x})}{\bar{x}}\right) \tag{4.7}$$

$$= \begin{cases} \dfrac{120}{\bar{x}^7} + \mathcal{O}\Big(\dfrac{1}{\bar{x}}\Big) & , \quad \bar{x} \ll 1 \\ \dfrac{24}{\bar{x}^6} + \mathcal{O}\Big(e^{-2\bar{x}}\Big) & , \quad \bar{x} \gg 1 \end{cases} \,. \tag{4.8}$$

The function $\phi_{\rm NLO}(\bar{x})$, which determines the long-distance asymptotics of the next-to-leading order correction, reads

$$\begin{aligned}
\phi_{\rm NLO}(\bar{x}) &= -\frac{4}{3\bar{x}^4} + \frac{24}{\bar{x}^5} + \frac{88}{\bar{x}^6}\Big[i(2\bar{x}) - \ln(2\bar{x})\Big] && (4.9)\\
&= \begin{cases} -\dfrac{64}{\bar{x}^5} + \dfrac{40}{3\bar{x}^4} + \mathcal{O}\Big(\dfrac{1}{\bar{x}^2}\Big) & , \quad \bar{x} \ll 1 \\ -\dfrac{4}{3\bar{x}^4} + \dfrac{24}{\bar{x}^5} - \dfrac{88\ln(2\bar{x})}{\bar{x}^6} + \mathcal{O}\Big(e^{-2\bar{x}}\Big) & , \quad \bar{x} \gg 1 \end{cases} . && (4.10)
\end{aligned}$$

The remaining functions ϕ_1 and ϕ_2 are subdominant at long distances (ϕ_1 by exponential terms, ϕ_2 by powerlike terms), and take the respective forms

$$\begin{aligned}
\phi_1(\bar{x}) &= \frac{80}{3\bar{x}^4}\, n(2\bar{x}) + \left[\frac{268}{\bar{x}^5} - \frac{24}{\bar{x}^3}\right] n'(2\bar{x}) + \left[-\frac{676}{3\bar{x}^4} + \frac{80}{3\bar{x}^2}\right] n''(2\bar{x}) \\
&+ \left[\frac{496}{9\bar{x}^3} - \frac{16}{\bar{x}}\right] n^{(3)}(2\bar{x}) + \frac{1072}{9\bar{x}^2}\, n^{(4)}(2\bar{x}) \\
&+ \frac{33}{9\bar{x}} \int_0^\infty \mathrm{d}\tilde{y}\, (2+\tilde{y})^4 \ln\left(\frac{2+\tilde{y}}{\tilde{y}}\right) n^{(5)}\Big((2+\tilde{y})\bar{x}\Big) \\
&+ \frac{1}{\bar{x}} \int_0^{\bar{x}} \mathrm{d}\bar{y} \left(\coth\bar{y} - \frac{1}{\bar{y}} - \frac{\bar{y}}{3}\right) \frac{\mathrm{d}^4}{\mathrm{d}\bar{x}^4} \left[\frac{\mathrm{Li}_3\left(e^{-2\bar{x}}\right) - \mathrm{Li}_3\left(e^{-2(\bar{x}+\bar{y})}\right)}{\bar{x}\bar{y}^3}\right. \\
&\quad \left. - \frac{\mathrm{Li}_2\left(e^{-2\bar{x}}\right) + \mathrm{Li}_2\left(e^{-2(\bar{x}+\bar{y})}\right)}{\bar{x}\bar{y}^2} + 4\,\frac{i(2(\bar{x}+\bar{y})) - i(2\bar{x})}{\bar{x}\bar{y}}\right] \\
&+ \frac{1}{\bar{x}} \int_{\bar{x}}^\infty \mathrm{d}\bar{y} \left(\coth\bar{y} - \frac{1}{\bar{y}} - \frac{\bar{y}}{3}\right) \frac{\mathrm{d}^4}{\mathrm{d}\bar{x}^4} \left[\frac{\mathrm{Li}_3\left(e^{-2\bar{y}}\right) - \mathrm{Li}_3\left(e^{-2(\bar{x}+\bar{y})}\right)}{\bar{x}\bar{y}^3}\right. \\
&\quad \left. + \frac{\mathrm{Li}_2\left(e^{-2\bar{y}}\right) - \mathrm{Li}_2\left(e^{-2(\bar{x}+\bar{y})}\right)}{\bar{x}\bar{y}^2} + 4\,\frac{i(2(\bar{x}+\bar{y})) - i(2\bar{y})}{\bar{x}\bar{y}}\right], \qquad (4.11)
\end{aligned}$$

$$\begin{aligned}
\phi_2(\bar{x}) &= \frac{1}{4\pi\bar{x}} \int_0^\infty \mathrm{d}\tilde{y}\, \mathrm{d}\tilde{z} \int_{-1}^1 \mathrm{d}t_1\, \mathrm{d}t_2 \int_0^{2\pi} \mathrm{d}\phi\, \frac{\tilde{y}\tilde{z}}{|\mathbf{e} - \tilde{\mathbf{y}}||\mathbf{e} - \tilde{\mathbf{z}}||\tilde{\mathbf{y}} - \tilde{\mathbf{z}}|} \\
&\quad \times \frac{\mathrm{d}^6}{\mathrm{d}\bar{x}^6}\left\{\bar{x}^2\Big[n(\bar{x}a) + 2n(\bar{x}b) + n(\bar{x}c)n(\bar{x}b) + 2n(\bar{x}a)n(\bar{x}b)\Big]\right\}, \qquad (4.12) \\
a &\equiv \tilde{y} + \tilde{z} + |\mathbf{e} - \tilde{\mathbf{y}}| + |\mathbf{e} - \tilde{\mathbf{z}}|\,, \quad b \equiv \tilde{y} + \tilde{z} + |\tilde{\mathbf{y}} - \tilde{\mathbf{z}}|\,, \quad c \equiv a + b - 2(\tilde{y} + \tilde{z})\,.
\end{aligned}$$

The integrals still remaining in the definitions of ϕ_1 and ϕ_2 are carried out numerically. The analytically known functions $\phi_{\rm LO}$, $\phi_{\rm NLO}$ are illustrated in fig. 2, the numerically determined functions ϕ_1, ϕ_2 in fig. 3.

Let us work out the asymptotic behaviours of ϕ_1 and ϕ_2. For ϕ_1, we find

$$\begin{aligned}
\phi_1^{\rm UV}(\bar{x}) &= -\frac{824}{3\bar{x}^7} + \frac{58}{\bar{x}^5} - \frac{40}{3\bar{x}^4} - \frac{1}{45\bar{x}^3} + \mathcal{O}\left(\frac{1}{\bar{x}^2}\right), \quad \bar{x} \ll 1\,, && (4.13)\\
\phi_1^{\rm IR}(\bar{x}) &= \mathcal{O}(e^{-2\bar{x}})\,, \quad \bar{x} \gg 1\,. && (4.14)
\end{aligned}$$

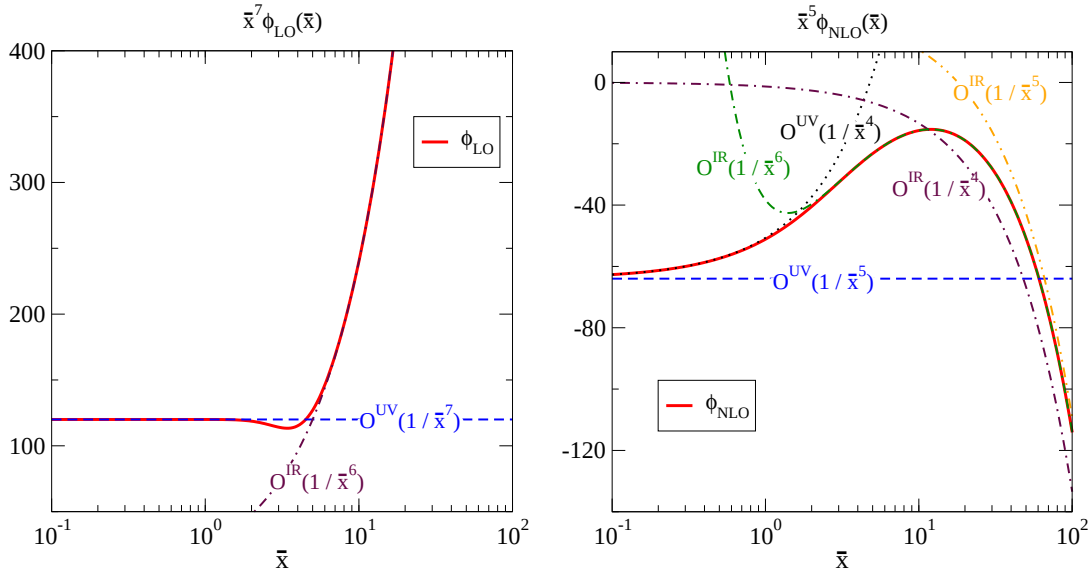

Figure 2: The basic functions defined in eqs. (4.7), (4.9), together with their asymptotic limits as given in eqs. (4.8), (4.10). The functions $O^{\rm UV/IR}$ indicate the nature of the limit, and the argument shows the order up to which terms have been included.

For ϕ_2, in turn, the short-distance behaviour is

$$\phi_2^{\rm UV}(\bar{x}) = \frac{6}{\bar{x}^5} + \frac{5}{27\bar{x}^3} + \mathcal{O}\left(\frac{1}{\bar{x}}\right), \quad \bar{x} \ll 1\,. \tag{4.15}$$

The infrared behaviour is, in contrast, rather non-trivial: while all terms in ϕ_1 are exponentially small at long distances, there are some parts in ϕ_2 which are not. Indeed, despite a large $\bar{x}$, there is a slice in the integration range of eq. (4.12) where b is small (because of the appearance of the unit vectors, this is not possible in the terms involving a or c). The intuitive meaning of this term is perhaps clearest if it is rewritten in momentum space:

$$\begin{aligned}\phi_2^{\rm IR}(\bar{x}) &\equiv \frac{1}{2\pi\bar{x}}\int_0^\infty \mathrm{d}\tilde{y}\,\mathrm{d}\tilde{z}\int_{-1}^1 \mathrm{d}t_1\,\mathrm{d}t_2\int_0^{2\pi}\mathrm{d}\phi\,\frac{\tilde{y}\tilde{z}}{|\mathbf{e}-\tilde{\mathbf{y}}||\mathbf{e}-\tilde{\mathbf{z}}||\tilde{\mathbf{y}}-\tilde{\mathbf{z}}|}\frac{\mathrm{d}^6}{\mathrm{d}\bar{x}^6}\left[\frac{\bar{x}^2}{e^{\bar{x}(\tilde{y}+\tilde{z}+|\tilde{\mathbf{y}}-\tilde{\mathbf{z}}|)}-1}\right] \\ &= \frac{4\,\nabla^6}{\pi^2 T^6}\int_{\mathbf{p}}\frac{e^{i\mathbf{p}\cdot\mathbf{x}}}{p^2}\int_{\mathbf{q}}\frac{e^{i\mathbf{q}\cdot\mathbf{x}}}{q^2}\sum\!\!\!\!\!\!\int_R{}'\,\frac{1}{R^2(q-R)^2(p+R)^2}\,.\end{aligned} \tag{4.16}$$

This corresponds to a contribution from graph (vii) of fig. 1 where a non-zero Matsubara mode circulates in one of the triangles; even if we shrink this "heavy-mode contribution" to a series of higher-order operators, there still remains an infrared contribution in which the remaining two propagators have Matsubara zero modes. These power-law contributions can be obtained by expanding the result of the sum-integral over R in powers of p and q and

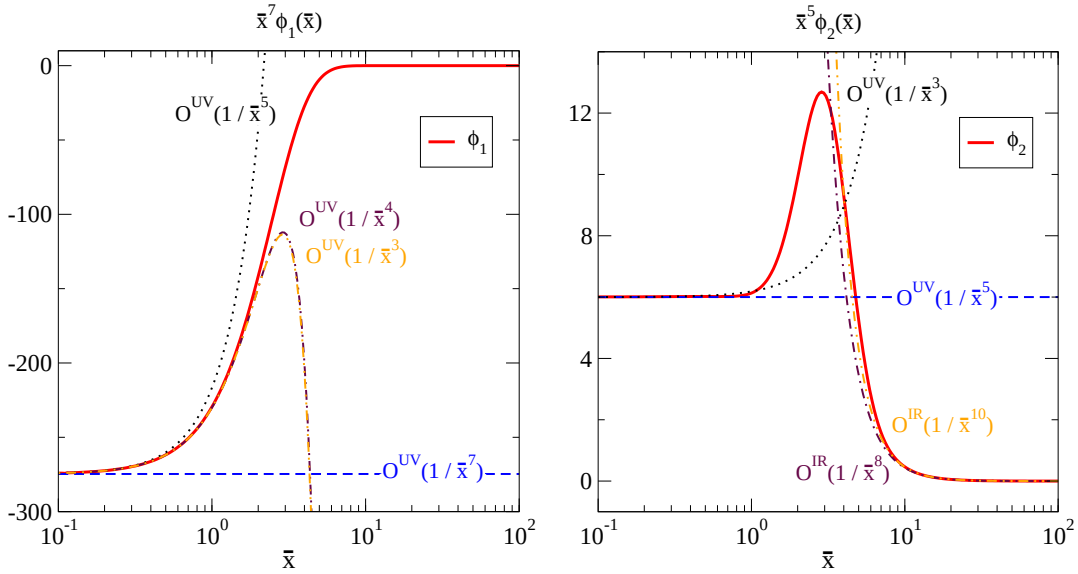

Figure 3: The basic functions defined in eqs. (4.11), (4.12), together with their asymptotic limits as given in eqs. (4.13), (4.15), (4.17). The functions $O^{\rm UV/IR}$ indicate the nature of the limit, and the argument shows the order up to which terms have been included.

omitting contact terms, which immediately leads to

$$\phi_2^{\rm IR}(\bar{x}) = \frac{360\zeta(3)}{\bar{x}^8} + \frac{2520\zeta(5)}{\bar{x}^{10}} + \mathcal{O}\biggl(\frac{1}{\bar{x}^{12}}\biggr) \;, \quad \bar{x} \gg 1 \;. \tag{4.17}$$

4.2. Asymptotic behaviours

Inserting the asymptotic expansions in eqs. (4.8), (4.10), (4.13), (4.14), (4.15), (4.17) into eqs. (4.5), (4.6), we can write down the asymptotic expansions for the functions $\bar{G}_\theta^{\rm F}$ and $\bar{G}_\chi^{\rm F}$ at small and large $\bar{x}$. In the short-distance limit we get

$$\begin{aligned} \frac{\bar{G}_\theta^{\rm F,UV}(x)}{4d_A c_\theta^2} &= \frac{g^4\pi^4T^7}{\bar{x}^7}\biggl\{480 + \frac{g^2N_{\rm c}}{\pi^2}\biggl[440\ln\bigl(e^{\gamma_{\rm E}}\bar{\Lambda}x\bigr) - \frac{824}{3}\biggr]\biggr\} \\ &\quad + \frac{22\,g^6N_{\rm c}\pi^2T^7}{135\bar{x}^3} + \mathcal{O}\biggl(\frac{g^4}{\bar{x}}, \frac{g^6}{\bar{x}}, \frac{g^8}{\bar{x}^7}\biggr) \;, \quad \bar{x} \ll 1 \;, \end{aligned} \tag{4.18}$$

$$\begin{aligned} \frac{\bar{G}_\chi^{\rm F,UV}(x)}{-16d_A c_\chi^2} &= \frac{g^4\pi^4T^7}{\bar{x}^7}\biggl\{480 + \frac{g^2N_{\rm c}}{\pi^2}\biggl[440\ln\bigl(e^{\gamma_{\rm E}}\bar{\Lambda}x\bigr) - \frac{104}{3}\biggr]\biggr\} \\ &\quad + \frac{22\,g^6N_{\rm c}\pi^2T^7}{135\bar{x}^3} + \mathcal{O}\biggl(\frac{g^4}{\bar{x}}, \frac{g^6}{\bar{x}}, \frac{g^8}{\bar{x}^7}\biggr) \;, \quad \bar{x} \ll 1 \;. \end{aligned} \tag{4.19}$$

Note that the dominant terms, i.e. the first rows, are temperature-independent. The expressions obtained agree with the OPE results that can be extracted from ref. [12], but two

features are worth stressing. First of all, the leading thermal correction is of $\mathcal{O}(g^6)$ and positive, whereas $\mathcal{O}(g^4)$ only gives a subleading thermal contribution at short distances; in equal-time correlators, in contrast, both orders contribute to the leading term $\mathcal{O}(-1/\bar{x}^4)$, which is negative at short distances [6, 12]. This drastic difference illustrates that averaging over the Euclidean time coordinate has a significant effect if $x \lesssim \beta$. Second, the OPE contributions proportional to $(e-3p)(T)$, which come with opposite signs in the two channels and distinguish them from each other [11, 12], are of $\mathcal{O}(g^8/\bar{x}^3)$ and thus beyond the accuracy of our present $\mathcal{O}(g^6)$ analysis.

At long distances, on the other hand, we obtain

$$\begin{aligned}
\frac{\bar{G}_\theta^{\mathrm{F,IR}}(x)}{4d_A c_\theta^2} &= g^4\pi^4T^7\left\{\frac{96}{\bar{x}^6} + \frac{g^2N_\mathrm{c}}{\pi^2}\left[-\frac{4}{3\bar{x}^4} + \frac{24}{\bar{x}^5} + \frac{88}{\bar{x}^6}\ln\frac{e^{\gamma_\mathrm{E}}\bar{\Lambda}}{4\pi T}\right]\right\} \\
&\quad + \frac{360\zeta(3)g^6N_\mathrm{c}\pi^2T^7}{\bar{x}^8} + \mathcal{O}\biggl(g^4e^{-2\bar{x}}, \frac{g^6}{\bar{x}^{10}}, \frac{g^8}{\bar{x}^2}\biggr)\,, \quad \bar{x} \gg 1\,, \qquad (4.20) \\
\frac{\bar{G}_\chi^{\mathrm{F,IR}}(x)}{-16d_A c_\chi^2} &= g^4\pi^4T^7\left\{\frac{96}{\bar{x}^6} + \frac{g^2N_\mathrm{c}}{\pi^2}\left[-\frac{4}{3\bar{x}^4} + \frac{24}{\bar{x}^5} + \frac{88}{\bar{x}^6}\left(\ln\frac{e^{\gamma_\mathrm{E}}\bar{\Lambda}}{4\pi T} + \frac{6}{11}\right)\right]\right\} \\
&\quad + \frac{360\zeta(3)g^6N_\mathrm{c}\pi^2T^7}{\bar{x}^8} + \mathcal{O}\biggl(g^4e^{-2\bar{x}}, \frac{g^6}{\bar{x}^{10}}, \frac{g^8}{\bar{x}^2}\biggr)\,, \quad \bar{x} \gg 1\,. \qquad (4.21)
\end{aligned}$$

The first rows indicate that at sufficiently large distances, $\bar{x}^2 \gg \pi^2/g^2N_\mathrm{c}$, the correction of $\mathcal{O}(g^6)$ overtakes the term of $\mathcal{O}(g^4)$; this signals a breakdown of the perturbative series and necessitates a resummation, to which we now turn.

5. Effective theory computation

As can be observed from eqs. (4.20), (4.21), at distances of the order $x^2 \sim 1/g^2T^2N_\mathrm{c}$ the naive perturbative series breaks down and needs to be resummed in order to recover the correct long-distance behaviour. A systematic way to implement these resummations is provided by effective theories. In our case the relevant low-energy effective theory is known as EQCD, a three-dimensional theory for the Matsubara zero modes of A_i^a and A_0^a [18, 19].

Keeping the dimensions of the fields as they are in the original theory, and continuing to denote by g^2 the renormalized 4d gauge coupling, the operators we are interested in can be represented in EQCD as

$$\theta^\mathrm{E} = c_\theta\, g^2\left[\mathcal{Z}_\mathrm{F}\tilde{F}_{ij}^a\tilde{F}_{ij}^a + 2\mathcal{Z}_\mathrm{D}(\mathcal{D}_i\tilde{A}_0)^a(\mathcal{D}_i\tilde{A}_0)^a + \ldots\right]\,, \qquad (5.1)$$

$$\chi^\mathrm{E} = c_\chi\, g^2\left[-4\mathcal{Z}_\mathrm{E}\,\epsilon_{ijk}\,(\mathcal{D}_i\tilde{A}_0)^a\tilde{F}_{jk}^a + \ldots\right]\,, \qquad (5.2)$$

where the numerical coefficients have been chosen so that the renormalization factors $\mathcal{Z}_\mathrm{F}$, $\mathcal{Z}_\mathrm{D}$, $\mathcal{Z}_\mathrm{E}$ are all of the form $1+\mathcal{O}(g^2)$. Dropping again contact terms, and setting $\epsilon = 0$ since

the contributions are ultraviolet finite, the leading-order results can be written as

$$\frac{\bar{G}_\theta^{\rm E}(x)}{4d_A c_\theta^2 g^4} = T\int_{\mathbf{p}} e^{i\mathbf{p}\cdot\mathbf{x}} \int_{\mathbf{q}} \biggl[\frac{\mathcal{Z}_{\rm F}^2}{2} \frac{p^4}{q^2(p-q)^2} + \frac{\mathcal{Z}_{\rm D}^2}{2} \frac{(p^2+2m_{\rm E}^2)^2}{(q^2+m_{\rm E}^2)[(p-q)^2+m_{\rm E}^2]} \biggr]$$
$$= \frac{\mathcal{Z}_{\rm F}^2 T}{2(4\pi)^2 x} \frac{{\rm d}^4}{{\rm d}x^4}\biggl(\frac{1}{x}\biggr) + \frac{\mathcal{Z}_{\rm D}^2 T}{2(4\pi)^2 x} \biggl(\frac{{\rm d}^2}{{\rm d}x^2} - 2m_{\rm E}^2\biggr)^2 \biggl(\frac{e^{-2m_{\rm E}x}}{x}\biggr)\,, \tag{5.3}$$

$$\frac{\bar{G}_\chi^{\rm E}(x)}{-16d_A c_\chi^2 g^4} = T\int_{\mathbf{p}} e^{i\mathbf{p}\cdot\mathbf{x}} \int_{\mathbf{q}} \frac{\mathcal{Z}_{\rm E}^2 (p^2+m_{\rm E}^2)^2}{(q^2+m_{\rm E}^2)(p-q)^2}$$
$$= \frac{\mathcal{Z}_{\rm E}^2 T}{(4\pi)^2 x} \biggl(\frac{{\rm d}^2}{{\rm d}x^2} - m_{\rm E}^2\biggr)^2 \biggl(\frac{e^{-m_{\rm E}x}}{x}\biggr)\,, \tag{5.4}$$

where $m_{\rm E}^2$ is the Debye mass parameter appearing in the EQCD Lagrangian. To avoid double-counting, we write the observables as

$$\bar{G}_{\theta,\chi}(x) = \Bigl[\bar{G}_{\theta,\chi}^{\rm F}(x) - \bar{G}_{\theta,\chi}^{\rm E}(x)\Bigr]_{\rm naive} + \Bigl[\bar{G}_{\theta,\chi}^{\rm E}(x)\Bigr]_{\rm resummed}\,, \tag{5.5}$$

where the quantity in the first square brackets is infrared safe. In the "naive" results, $m_{\rm E}$ is treated as a perturbatively small quantity of $\mathcal{O}(g)$, and we can expand with respect to it in eqs. (5.3), (5.4), giving

$$\biggl(\frac{\bar{G}_\theta^{\rm E}(x)}{4d_A c_\theta^2 g^4}\biggr)_{\rm naive} = \mathcal{Z}_{\rm F}^2 \biggl[\frac{48\pi^4 T^7}{\bar{x}^6}\biggr] + \mathcal{Z}_{\rm D}^2 \biggl[\frac{48\pi^4 T^7}{\bar{x}^6} - \frac{4\pi^2 T^5 m_{\rm E}^2}{\bar{x}^4} + \mathcal{O}\Bigl(m_{\rm E}^4\Bigr)\biggr]\,, \tag{5.6}$$

$$\biggl(\frac{\bar{G}_\chi^{\rm E}(x)}{-16d_A c_\chi^2 g^4}\biggr)_{\rm naive} = \mathcal{Z}_{\rm E}^2 \biggl[\frac{96\pi^4 T^7}{\bar{x}^6} - \frac{4\pi^2 T^5 m_{\rm E}^2}{\bar{x}^4} + \mathcal{O}\Bigl(m_{\rm E}^4\Bigr)\biggr]\,. \tag{5.7}$$

Substituting $m_{\rm E}^2 = g^2 T^2 N_{\rm c}/3$, $\mathcal{Z}_{\rm F} = \mathcal{Z}_{\rm D} = \mathcal{Z}_{\rm E} = 1$ and comparing with eqs. (4.20) and (4.21), we see that these reproduce the dominant LO and NLO long-distance behaviours. Therefore, in both channels, the subtraction-addition step of eq. (5.5) replaces the leading infrared contribution $\sim -g^6 N_{\rm c}/\bar{x}^4$ by an exponentially suppressed behaviour, proportional to $\sim \exp(-m_{\rm E}x)$ in the pseudoscalar (χ) and to $\sim \exp(-2m_{\rm E}x)$ in the scalar (θ) channel, thereby postponing the breakdown of the perturbative series to larger distances.

As far as the subleading infrared terms are concerned, we would expect those of $\mathcal{O}(g^6 N_{\rm c}/\bar{x}^5)$ to also be replaced by exponentially suppressed terms in the pseudoscalar channel (χ), in which symmetries require the appearance of an odd number of $\tilde{A}_0^a$ propagators in any intermediate state [5]. (In other words, the effective theory for the static colour-magnetic modes, MQCD, does not contain operators with the right quantum numbers to contribute to $\bar{G}_\chi$.) In contrast, in the scalar channel, power-law terms of $\mathcal{O}(g^6 N_{\rm c}/\bar{x}^5)$ remain over, and imply that our computation becomes unreliable at the distance scale where this term overtakes the leading-order term, i.e. when $\mathcal{O}(1/\bar{x}^6) \sim \mathcal{O}(g^2 N_{\rm c}/\pi^2 \bar{x}^5)$. This happens at the non-perturbative colour-magnetic scale $x \sim \pi/(g^2 N_{\rm c} T)$; the corresponding behaviour could in principle be determined through a non-perturbative analysis of MQCD.

As far as the remaining power-law terms go, those of $\mathcal{O}(g^6 N_{\rm c} T^7/\bar{x}^6)$ could be accounted for by a choice of the $\mathcal{O}(g^2)$ corrections to the renormalization factors $\mathcal{Z}_{\rm F}, \mathcal{Z}_{\rm D}, \mathcal{Z}_{\rm E}$. Unfortunately, our present results do not suffice to fix all of these unambigously, but further matching computations would be needed. Higher powers still, $\mathcal{O}(g^6 T^7/\bar{x}^8)$ etc, correspond to higher-dimensional operators within EQCD or MQCD. Since the focus of the present paper is on intermediate distances, we have not carried out a next-to-leading order analysis of the correlators on the EQCD side. Rather, we will use leading-order resummation, as implied by eqs. (5.3)–(5.7), to gauge the distance scale where infrared effects become important, and declare our results as unreliable above this scale. Explicitly, our resummation amounts to the additional contributions

$$\frac{\delta_{\rm resum}\bar{G}_\theta(x)}{4d_A c_\theta^2} = -g^4\pi^4 T^7\biggl[\frac{48}{\bar{x}^6} - \frac{4g^2 N_{\rm c}}{3\pi^2\bar{x}^4}\biggr] + \frac{g^4 m_{\rm E}^6 T}{32\pi^2\tilde{x}}\biggl(\frac{{\rm d}^2}{{\rm d}\tilde{x}^2} - 2\biggr)^2\biggl(\frac{e^{-2\tilde{x}}}{\tilde{x}}\biggr)\,, \tag{5.8}$$

$$\frac{\delta_{\rm resum}\bar{G}_\chi(x)}{-16d_A c_\chi^2} = -g^4\pi^4 T^7\biggl[\frac{96}{\bar{x}^6} - \frac{4g^2 N_{\rm c}}{3\pi^2\bar{x}^4}\biggr] + \frac{g^4 m_{\rm E}^6 T}{16\pi^2\tilde{x}}\biggl(\frac{{\rm d}^2}{{\rm d}\tilde{x}^2} - 1\biggr)^2\biggl(\frac{e^{-\tilde{x}}}{\tilde{x}}\biggr)\,, \tag{5.9}$$

to be added to eqs. (4.5), (4.6), with $\tilde{x} \equiv m_{\rm E} x$.

6. Numerical evaluation

6.1. Choice of the renormalization scale

Upon adding together the full theory and EQCD contributions to the correlators, eqs. (4.5) and (5.8) for the θ channel and eqs. (4.6) and (5.9) for the χ channel, we are now ready to numerically estimate the behaviour of the functions in various regimes. We do this for a variety of distance scales, ranging from $x \ll 1/\pi T$ to $x \gg 1/\pi T$, which in particular implies that we should choose an "optimal" renormalization scale that adapts to the physical quantity and distance regime of interest. At short distances, it is natural to determine the optimal scale from the UV limit of the correlators, demanding that the leading $\bar{\Lambda}$-dependent term in the NLO part of the results vanishes. According to eqs. (4.18) and (4.19) this yields

$$\bar{\Lambda}_\theta^x = \frac{e^{103/165-\gamma_{\rm E}}}{x}\,, \quad \bar{\Lambda}_\chi^x = \frac{e^{13/165-\gamma_{\rm E}}}{x}\,. \tag{6.1}$$

At long distances, on the other hand, we fix the scale from the logarithmic terms in eqs. (4.20), (4.21), which correspond to NLO corrections to the factors $\mathcal{Z}_{\rm F}, \mathcal{Z}_{\rm D}, \mathcal{Z}_{\rm E}$ of sec. 5 and are not otherwise cancelled by the resummation. This gives

$$\bar{\Lambda}_\theta^T = e^{-\gamma_{\rm E}}\,4\pi T\,, \quad \bar{\Lambda}_\chi^T = e^{-6/11-\gamma_{\rm E}}\,4\pi T\,. \tag{6.2}$$

(Remarkably, in both channels, the short-distance and long-distance scale choices coincide at $\bar{x} = e^{103/165-\ln 2} \approx 0.9334$.) At intermediate distances, we make the simple choice of defining

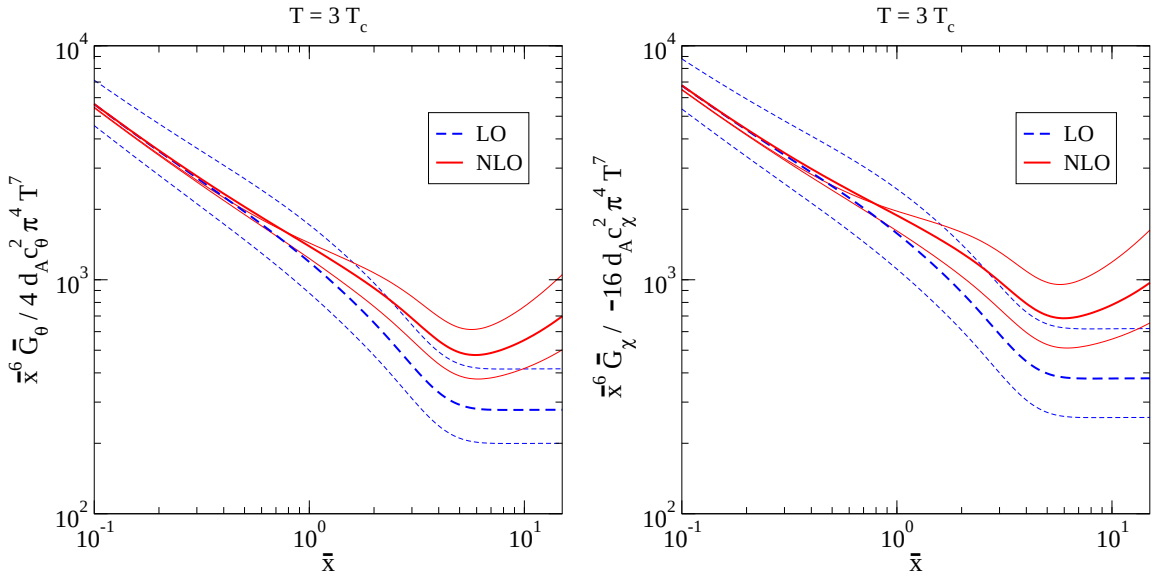

Figure 4: The behaviour of the full θ (left) and χ (right) correlators, multiplied by $\bar{x}^6$, at $T = 3T_{\rm c}$. Thick lines indicate the scale choice $\bar{\Lambda} = \bar{\Lambda}^{\rm opt}$ (eq. (6.3)), thin lines variations by a factor of 2 around this scale. Both correlators vary rapidly with $\bar{x}$ and are dominated by a vacuum-like behaviour up to distances $\bar{x} \sim$ a few. Our results become inaccurate at $\bar{x} \gtrsim 10$, cf. fig. 8.

an "optimal" scale through

$$\bar{\Lambda}^{\rm opt} \quad \equiv \quad \sqrt{(\bar{\Lambda}^T)^2 + (\bar{\Lambda}^x)^2}\,. \tag{6.3}$$

Subsequently we vary our $\bar{\Lambda}$ parameter by a factor of 2 around this scale.

As far as the gauge coupling is concerned, we solve it from the 2-loop renormalization group equation, and define

$$\Lambda_{\overline{\rm MS}} \equiv \lim_{\bar{\Lambda}\to\infty} \bar{\Lambda} \Big(b_0 g^2\Big)^{-b_1/2b_0^2} \exp\bigg(-\frac{1}{2b_0 g^2}\bigg)\,. \tag{6.4}$$

Where needed, the Debye mass parameter is evaluated from the leading-order expression $m_{\rm E}^2 = g^2 T^2 N_{\rm c}/3$ with the same g^2 inserted as elsewhere.

6.2. Plots

We start by inspecting the behaviour of the full correlators over a wide distance range. This leads to the plots shown in figs. 4, 5 where we display

$$\frac{\bar{G}_\theta(x)}{4 d_A c_\theta^2\, \pi^4 T^7} \qquad \text{and} \qquad \frac{\bar{G}_\chi(x)}{-16 d_A c_\chi^2\, \pi^4 T^7}\,, \tag{6.5}$$

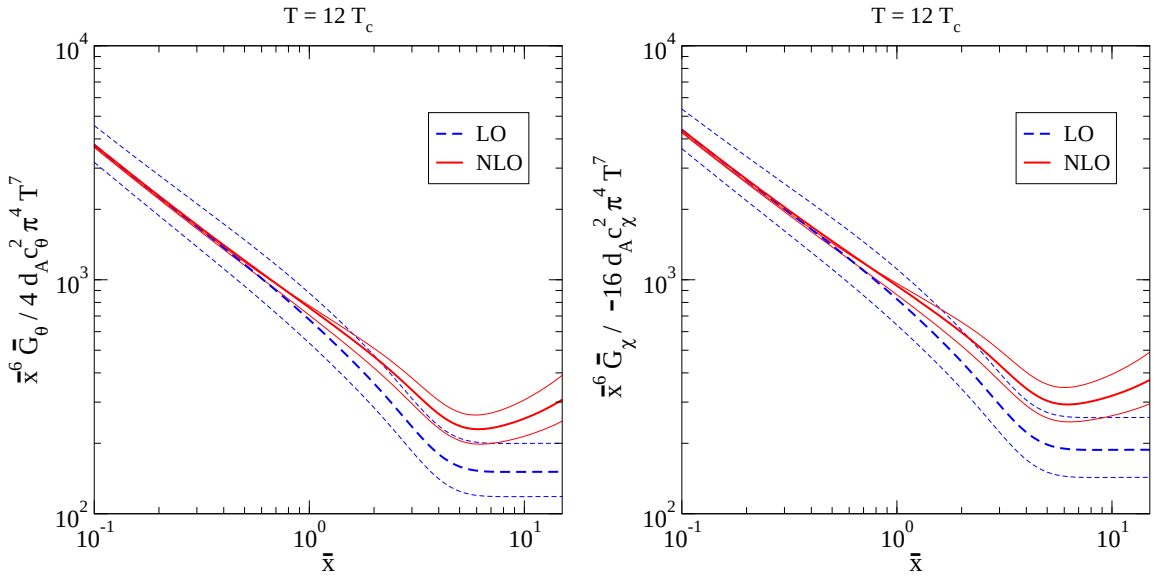

Figure 5: Like fig. 4 but at $T = 12T_{\rm c}$.

multiplied by $\bar{x}^6$ in order to increase the resolution, on a log-log scale at the temperatures $T = 3T_{\rm c}$ ($T_{\rm c} \equiv 1.25\Lambda_{\overline{\rm MS}}$) and $T = 12T_{\rm c}$ for $\bar{\Lambda} = n\,\bar{\Lambda}^{\rm opt}$, $n = \frac{1}{2}, 1, 2$. A power-law behaviour can be clearly observed at short distances, whereas the dependence of the result on the renormalization scale as well as the magnitude of the NLO correction become visible at long distances, indicating that the perturbative series becomes less trustworthy there.

In order to observe more clearly the fine structures of the correlators, we next consider the functions

$$\frac{\Delta\bar{G}_\theta(x)}{4d_A c_\theta^2\,\pi^4 T^7} \equiv \frac{\bar{G}_\theta(x) - \bar{G}_\theta^{\text{“vac”}}(x)}{4d_A c_\theta^2\,\pi^4 T^7}\,, \tag{6.6}$$

$$\frac{\Delta\bar{G}_\chi(x)}{-16d_A c_\chi^2\,\pi^4 T^7} \equiv \frac{\bar{G}_\chi(x) - \bar{G}_\chi^{\text{“vac”}}(x)}{-16d_A c_\chi^2\,\pi^4 T^7}\,. \tag{6.7}$$

Here the vacuum-like parts are *defined* through the first lines of eqs. (4.18), (4.19) with a particular scale choice:

$$\frac{\bar{G}_\theta^{\text{“vac”}}(x)}{4d_A c_\theta^2} \equiv \frac{g^4\pi^4}{(2\pi x)^7}\left\{480 + \frac{g^2 N_{\rm c}}{\pi^2}\left[440\ln\left(e^{\gamma_{\rm E}}\bar{\Lambda}x\right) - \frac{824}{3}\right]\right\}_{\bar{\Lambda}=n\,\bar{\Lambda}^{\rm opt}}\,, \tag{6.8}$$

$$\frac{\bar{G}_\chi^{\text{“vac”}}(x)}{-16d_A c_\chi^2} \equiv \frac{g^4\pi^4}{(2\pi x)^7}\left\{480 + \frac{g^2 N_{\rm c}}{\pi^2}\left[440\ln\left(e^{\gamma_{\rm E}}\bar{\Lambda}x\right) - \frac{104}{3}\right]\right\}_{\bar{\Lambda}=n\,\bar{\Lambda}^{\rm opt}}\,. \tag{6.9}$$

Although it would be tempting to interpret these as genuine vacuum results, this is not correct within our fixed-order computation: the genuine vacuum results become non-perturbative at a distance $x \sim 0.1$ fm and this is reflected by the fact that with the scale choices of eq. (6.1)

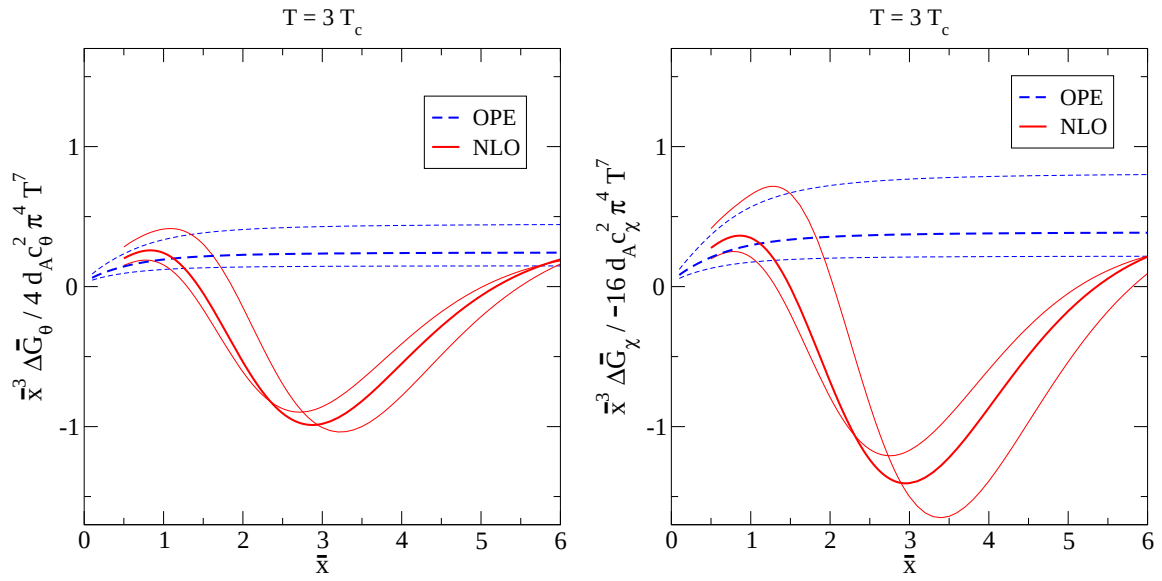

Figure 6: The short-distance behaviours of the "thermal" parts of the θ (left) and χ (right) correlators, multiplied by $\bar{x}^3$, compared with the corresponding OPE limits (the second lines of eqs. (4.18), (4.19)), at $T = 3T_c$. Thick lines indicate the scale choice $\bar{\Lambda} = \bar{\Lambda}^{\rm opt}$, thin lines variations by a factor of 2 around this scale. (Numerical evaluation is challenging at $\bar{x} \ll 1$ due to significance loss: not only the "vacuum" parts $1/\bar{x}^7$ but also "thermal" parts behaving as $1/\bar{x}^5$ and $1/\bar{x}^4$ cancel in $\Delta\bar{G}_{\theta,\chi}$ at $\bar{x} \lesssim 1$, cf. eqs. (4.10), (4.13), (4.15)).

the perturbative corrections grow out of control at $x \gtrsim 0.1\,\Lambda_{\overline{\rm MS}}^{-1}$ [12]. In contrast, in the full finite-temperature results of eq. (6.5) a scale choice like that in eq. (6.3) is well-motivated, and at sufficiently high temperatures the result is perturbative (apart from MQCD contributions) even at distances $x \sim$ fm. The definitions of eqs. (6.6)–(6.9) therefore only serve purposes of illustration. In any case, in figs. 6–8 these functions are plotted on various distance scales.

Considering first the UV limits of the correlators, in fig. 6 we display our results for $\Delta\bar{G}_\theta$ and $\Delta\bar{G}_\chi$ multiplied by $\bar{x}^3$, with $\bar{x}$ ranging from 0 to 6, and compare the results with the UV-limits in eqs. (4.18), (4.19). The results indicate that OPE-expanded results are applicable only in the range $\bar{x} \lesssim 1$, and that there is a visible difference between the two channels in the regime $1 \lesssim \bar{x} \lesssim 5$.

Next, motivated by the results of ref. [6], we inspect intermediate distances, $3 \leq \bar{x} \leq 12$. The results are plotted in fig. 7. The results suggest that the two channels are rather close to each other in the distance range $5 \lesssim \bar{x} \lesssim 10$.

Finally, fig. 8 shows the long-distance behaviours of $\Delta\bar{G}_\theta$ and $\Delta\bar{G}_\chi$ multiplied by $\bar{x}^5$ (so that, within our approximation, they approach constants at large $\bar{x}$). We compare the curves to the result of a calculation where no resummation of the soft modes was carried out. We observe that the $-1/\bar{x}^4$ behaviour of the unresummed result becomes fully visible only when

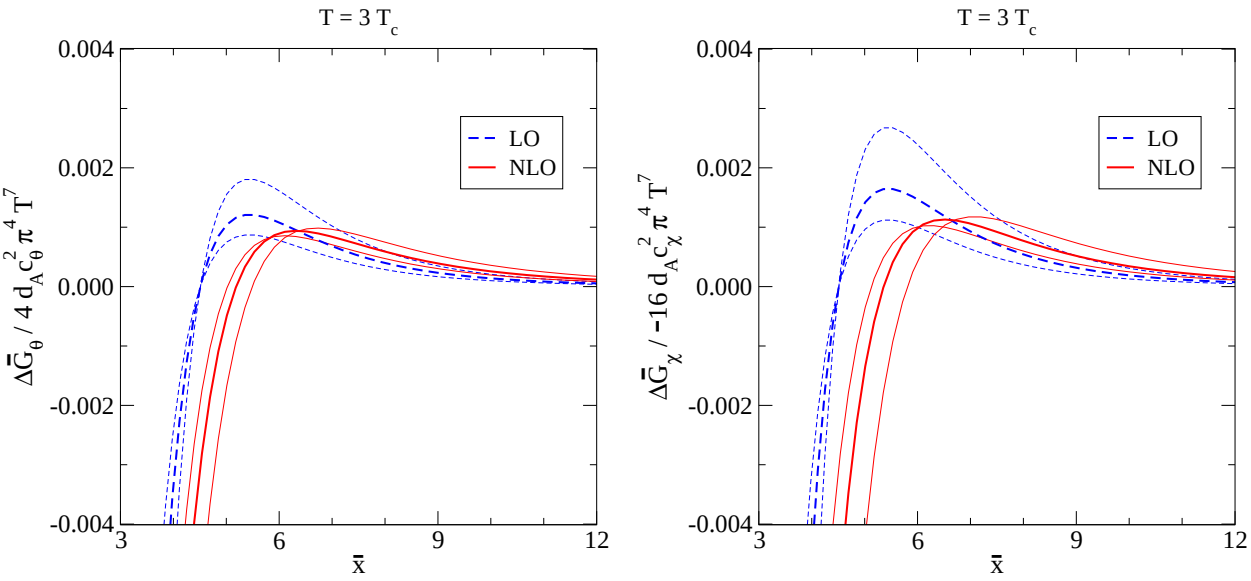

Figure 7: The "thermal" parts of the θ (left) and χ (right) correlators at intermediate distances, at $T = 3T_{\rm c}$. Thick lines indicate the scale choice $\bar{\Lambda} = \bar{\Lambda}^{\rm opt}$, thin lines variations by a factor of 2 around this scale. Correlations are slightly more pronounced in the χ channel.

$\bar{x} \gtrsim 10$. Further higher order or non-perturbative corrections, which would eventually turn the behaviour in both channels into exponential decay [5], can be assumed to become significant in the same range where resummation starts to dominate the behaviour, i.e. $\bar{x} \gtrsim 10$ at this temperature.

7. Conclusions

The purpose of this paper has been to "interpolate" between previous studies of the spatial correlation functions related to the operators $\theta \propto {\rm Tr}\,[F_{\mu\nu}F_{\mu\nu}]$ and $\chi \propto {\rm Tr}\,[F_{\mu\nu}\tilde{F}_{\mu\nu}]$ within pure SU(3) gauge theory at a finite temperature $T \sim$ a few $\times\, T_{\rm c}$. We find that the "ultraviolet limit", studied in ref. [12] (following refs. [6, 20] and other recent works), in which the correlators are computed with Operator Product Expansion type methods, works reasonably only at distances $2\pi T x \lesssim 1$ (cf. fig. 6). At the same time the "infrared limit", studied in ref. [5] and many subsequent works, starts to govern the behaviour at distances $2\pi T x \gtrsim 10$ (cf. fig. 8). In between, neither of these simplified approaches is viable, and our results represent the most precise weak-coupling expressions available to date. Whether they themselves are quantitatively accurate remains to be seen, once lattice measurements for the very same quantities, following the lines that have recently been published in ref. [6], become available.

Among the more detailed motivations of our study was the question, to what extent do the

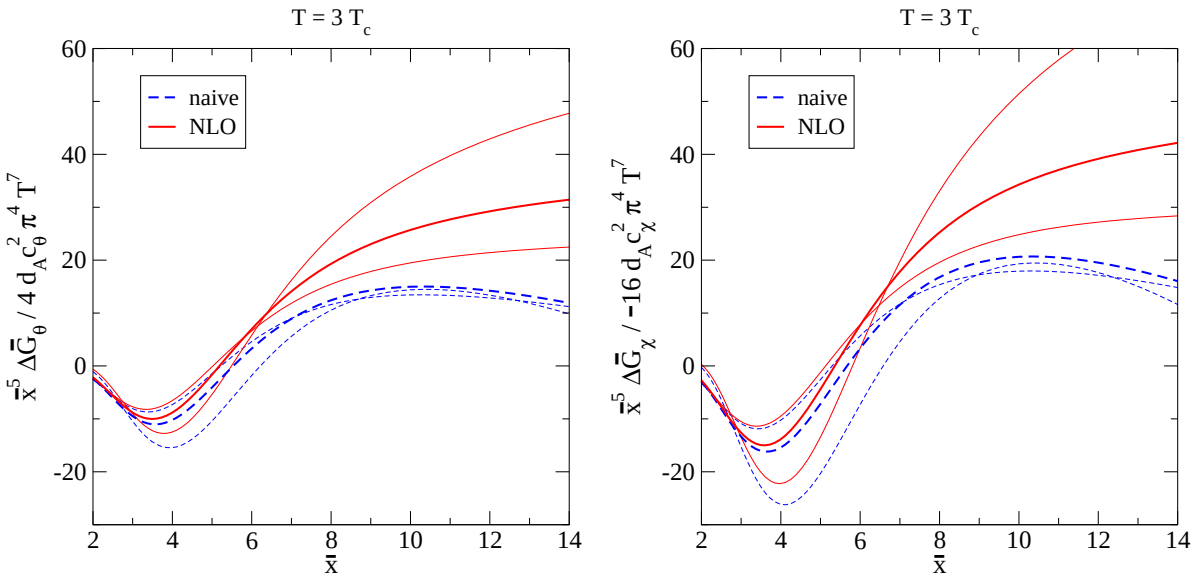

Figure 8: The long-distance behaviours of the θ (left) and χ (right) correlators, multiplied by $\bar{x}^5$, at $T = 3T_{\rm c}$. The results are compared with the "naive" expressions which do not include the resummations of eqs. (5.8), (5.9). Thick lines indicate the scale choice $\bar{\Lambda} = \bar{\Lambda}^{\rm opt}$, thin lines variations by a factor of 2 around this scale. The "naive" results become negative at long distances, whereas the resummed results remain positive and behave as $\sim 1/\bar{x}^5$ within our approximation. (This would turn into an exponential decay by higher order EQCD corrections or by non-perturbative MQCD effects.)

two correlators differ from each other? While we have indeed found some disparities between the two channels, in the direction that all features are more pronounced in the correlator corresponding to $\mathrm{Tr}\,[F_{\mu\nu}\tilde{F}_{\mu\nu}]$, the difference is not as striking as that seen in the lattice study of ref. [6]. Several possible reasons come to mind. First of all, the leading "conformality-breaking" OPE contribution proportional to $(e-3p)(T)$, showing a clear distinction between the two channels at short distances, corresponds actually to the 3-loop order in terms of Feynman graphs (in ref. [12] it could be "guessed" from the 2-loop computation carried out, by making use of renormalization scale invariance in connection with the general factorization philosophy inherent to OPE). This might suggest that 3-loop contributions are important insofar as the difference between the two channels is concerned. Second, it must be kept in mind that the lattice measurements in ref. [6] concerned strictly local correlators, whereas ours have been averaged over the Euclidean time coordinate. This has an important effect at least at distances $x \lesssim \beta$, i.e. $2\pi T x \lesssim$ a few. It will be interesting to repeat the comparison if lattice results for time-averaged correlators become available. Third, it should be stressed than in ref. [6] the genuine vacuum parts were subtracted from the thermal correlators. Unfortunately, this makes the difference sensitive to confinement physics; the features seen may *not* be a reflection of perturbative thermal physics alone. It would be useful to carry

out future comparisons *without* such a subtraction, i.e. directly with figs. 4, 5.

Let us remark that the "thermal" parts of the correlators, as well as the difference between the two "thermal" parts, show a remarkably rich x-dependence, suggesting that a high resolution is needed for disentangling all relevant features. As can be observed in figs. 6–8, the "thermal" parts change sign twice, before finally showing a positive correlation at long distances. At the same time, the difference between the two "thermal" parts, proportional to the thermal part of the function $\phi_{\rm LO}$ (cf. eq. (4.6) and fig. 2), shows the same two sign changes at short and intermediate distances, but would have a third one in store for long distances: at the "realistic" temperatures considered, the screening mass corresponding to $\mathrm{Tr}\,[F_{\mu\nu}\tilde{F}_{\mu\nu}]$ is markedly larger than that corresponding to $\mathrm{Tr}\,[F_{\mu\nu}F_{\mu\nu}]$ (cf. refs. [13, 14]), implying that at very large distances the correlator $\bar{G}_\chi$ would be smaller in magnitude than $\bar{G}_\theta$.

We end by recalling the relation of our work to heavy quarkonium physics and simultaneously the physical reason for considering time-averaged correlators as we have done in the present study. Whereas it was traditionally thought that heavy quarkonium melting is primarily a consequence of colour-electric Debye screening at long distances, $x \sim 1/gT$, it has been suggested in recent years that at least in the bottomonium case, where weak-coupling techniques are expected to be semi-quantitatively applicable, the "melting" of quarkonium resonances takes place already when the Bohr radius of the bound state, r, is parametrically in the range $1/\pi T \ll r \ll 1/gT$ [21]–[24]. In this situation the dominant mechanism for melting is not Debye screening but Landau damping or, more physically, the decoherence of the quantum mechanical bound state, mathematically represented by an imaginary part in the real-time static potential felt by a heavy quark-antiquark pair propagating in Minkowski time [25] (see also refs. [26]–[29]). Moreover, it can be argued that it is interesting to study quarkonium states even before they melt, whence the regime $x \lesssim 1/\pi T$ becomes relevant as well [30]. With such motivations, the "singlet free energy" as determined from lattice simulations [31] and traditionally used in potential models has recently been compared with perturbation theory at intermediate distances $x \sim 1/\pi T$, and a surprising agreement between the two was found [32].[1] The singlet free energy consists precisely of a correlator of two time-integrated objects. It is for this reason that we suspect time-averaged correlators to be of more direct physical relevance than strictly local ones. By learning about the reliability of the weak-coupling expansion for observables of this type in the intermediate distance range, it will hopefully become possible in the end to relate perturbative determinations of heavy quarkonium spectral functions (ref. [34] and references therein), which use the real-time static potential as input, to on-going lattice studies such as those in refs. [35, 36], thereby learning about the systematic errors on both sides.

[1] A similar if inequivalent observable, the correlator of two "traced" Polyakov loops, sometimes referred to as (exponent of minus) the "colour-averaged potential", was computed perturbatively in ref. [33], but no numerical evaluation or comparison with lattice data was presented.

Acknowledgements

We thank K. Kajantie and H.B. Meyer for useful discussions. M.L. was partly supported by the BMBF under project *Heavy Quarks as a Bridge between Heavy Ion Collisions and QCD*; M.V. was supported by the Academy of Finland, contract no. 128792, and A.V. by the Sofja Kovalevskaja program of the Alexander von Humboldt foundation.

References

[1] T.A. DeGrand and C.E. DeTar, *Static screening lengths in the gluon plasma,* Phys. Rev. D 34 (1986) 2469.

[2] C.E. DeTar and J.B. Kogut, *Measuring the Hadronic Spectrum of the Quark Plasma,* Phys. Rev. D 36 (1987) 2828.

[3] Y. Maezawa *et al.* [WHOT-QCD Collaboration], *Electric and Magnetic Screening Masses at Finite Temperature from Generalized Polyakov-Line Correlations in Two-flavor Lattice QCD,* Phys. Rev. D 81 (2010) 091501 [1003.1361].

[4] M. Cheng *et al.*, *Meson screening masses from lattice QCD with two light and the strange quark,* 1010.1216.

[5] P.B. Arnold and L.G. Yaffe, *The Non-Abelian Debye screening length beyond leading order,* Phys. Rev. D 52 (1995) 7208 [hep-ph/9508280].

[6] N. Iqbal and H.B. Meyer, *Spatial correlators in strongly coupled plasmas,* JHEP 11 (2009) 029 [0909.0582].

[7] P. Romatschke and D.T. Son, *Spectral sum rules for the quark-gluon plasma,* Phys. Rev. D 80 (2009) 065021 [0903.3946].

[8] H.B. Meyer, *The Bulk Channel in Thermal Gauge Theories,* JHEP 04 (2010) 099 [1002.3343].

[9] D.T. Son and A.O. Starinets, *Minkowski-space correlators in AdS/CFT correspondence: Recipe and applications,* JHEP 09 (2002) 042 [hep-th/0205051].

[10] A.L. Kataev, N.V. Krasnikov and A.A. Pivovarov, *Two-loop calculations for the propagators of gluonic currents,* Nucl. Phys. B 198 (1982) 508 [Erratum-ibid. B 490 (1997) 505] [hep-ph/9612326].

[11] V.A. Novikov, M.A. Shifman, A.I. Vainshtein and V.I. Zakharov, *Operator Expansion in Quantum Chromodynamics Beyond Perturbation Theory,* Nucl. Phys. B 174 (1980) 378.

[12] M. Laine, M. Vepsäläinen and A. Vuorinen, *Ultraviolet asymptotics of scalar and pseudoscalar correlators in hot Yang-Mills theory,* JHEP 10 (2010) 010 [1008.3263].

[13] A. Hart, M. Laine and O. Philipsen, *Static correlation lengths in QCD at high temperatures and finite densities,* Nucl. Phys. B 586 (2000) 443 [hep-ph/0004060].

[14] M. Laine and M. Vepsäläinen, *On the smallest screening masses in hot QCD,* JHEP 09 (2009) 023 [0906.4450].

[15] P.B. Arnold and C. Zhai, *The three loop free energy for pure gauge QCD,* Phys. Rev. D 50 (1994) 7603 [hep-ph/9408276].

[16] A. Gynther, M. Laine, Y. Schröder, C. Torrero and A. Vuorinen, *Four-loop pressure of massless O(N) scalar field theory,* JHEP 04 (2007) 094 [hep-ph/0703307].

[17] J. Möller and Y. Schröder, *Open problems in hot QCD,* 1007.1223.

[18] P. Ginsparg, *First and second order phase transitions in gauge theories at finite temperature,* Nucl. Phys. B 170 (1980) 388.

[19] T. Appelquist and R.D. Pisarski, *High-temperature Yang-Mills theories and three-dimensional Quantum Chromodynamics,* Phys. Rev. D 23 (1981) 2305.

[20] S. Caron-Huot, *Asymptotics of thermal spectral functions,* Phys. Rev. D 79 (2009) 125009 [0903.3958].

[21] Y. Burnier, M. Laine and M. Vepsäläinen, *Heavy quarkonium in any channel in resummed hot QCD,* JHEP 01 (2008) 043 [0711.1743].

[22] M.A. Escobedo and J. Soto, *Non-relativistic bound states at finite temperature: the hydrogen atom,* Phys. Rev. A 78 (2008) 032520 [0804.0691].

[23] M. Laine, *How to compute the thermal quarkonium spectral function from first principles?,* Nucl. Phys. A 820 (2009) 25C [0810.1112].

[24] F. Dominguez and B. Wu, *On dissociation of heavy mesons in a hot quark-gluon plasma,* Nucl. Phys. A 818 (2009) 246 [0811.1058].

[25] M. Laine, O. Philipsen, P. Romatschke and M. Tassler, *Real-time static potential in hot QCD,* JHEP 03 (2007) 054 [hep-ph/0611300].

[26] M. Laine, O. Philipsen and M. Tassler, *Thermal imaginary part of a real-time static potential from classical lattice gauge theory simulations,* JHEP 09 (2007) 066 [0707.2458].

[27] A. Beraudo, J.P. Blaizot and C. Ratti, *Real and imaginary-time $Q\bar{Q}$ correlators in a thermal medium,* Nucl. Phys. A 806 (2008) 312 [0712.4394].

[28] N. Brambilla, J. Ghiglieri, A. Vairo and P. Petreczky, *Static quark-antiquark pairs at finite temperature,* Phys. Rev. D 78 (2008) 014017 [0804.0993].

[29] A. Rothkopf, T. Hatsuda and S. Sasaki, *Proper heavy-quark potential from a spectral decomposition of the thermal Wilson loop,* PoS LAT2009 (2009) 162 [0910.2321].

[30] N. Brambilla, M.A. Escobedo, J. Ghiglieri, J. Soto and A. Vairo, *Heavy Quarkonium in a weakly-coupled quark-gluon plasma below the melting temperature,* JHEP 09 (2010) 038 [1007.4156].

[31] O. Kaczmarek, F. Karsch, P. Petreczky and F. Zantow, *Heavy Quark Anti-Quark Free Energy and the Renormalized Polyakov Loop,* Phys. Lett. B 543 (2002) 41 [hep-lat/0207002].

[32] Y. Burnier, M. Laine and M. Vepsäläinen, *Dimensionally regularized Polyakov loop correlators in hot QCD,* JHEP 01 (2010) 054 [0911.3480].

[33] N. Brambilla, J. Ghiglieri, P. Petreczky and A. Vairo, *Polyakov loop and correlator of Polyakov loops at next-to-next-to-leading order,* Phys. Rev. D 82 (2010) 074019 [1007.5172].

[34] Y. Burnier, M. Laine and M. Vepsäläinen, *Heavy quark medium polarization at next-to-leading order,* JHEP 02 (2009) 008 [0812.2105].

[35] G. Aarts, S. Kim, M.P. Lombardo, M.B. Oktay, S.M. Ryan, D.K. Sinclair and J.I. Skullerud, *Bottomonium above deconfinement in lattice nonrelativistic QCD,* 1010.3725.

[36] H.T. Ding, A. Francis, O. Kaczmarek, F. Karsch, H. Satz and W. Soeldner, *Charmonium correlation and spectral functions at finite temperature,* 1011.0695.